https://doi.org/10.5194/egusphere-2025-2331
Preprint. Discussion started: 25 June 2025

Exploring biogenic secondary organic aerosol using a PTRMS-CHARON in laboratory experiments: characterization and fingerprint analysis

Carolina Ramírez-Romero[1,2,a], Olatunde Murana[2], Hichem Bouzidi[2,b], Marina Jamar[2], Sébastien Dusanter[2], Alexandre Tomas[2], Ahmad Lahib[2,c],Layal Fayad[2,d], Véronique Riffault[2], Christopher Pöhlker[1], Stéphane Sauvage[2], and Joel F. de Brito[2]

[1]Multiphase Chemistry Department, Max Planck Institute for Chemistry, 55128 Mainz, Germany
[2]IMT Nord Europe, Institut Mines-Télécom, Université de Lille, Centre for Energy and Environment, 59000 Lille, France

[a] now at: Department of Chemistry, University of Toronto, Toronto, Canada
[b] now at: Université Paris Cité and Univ Paris Est Creteil, CNRS, LISA, F-75013 Paris, France
[c] now at: GRIMM Aerosol Technik, Ainring, Germany
[d] now at: Aix Marseille Univ, CNRS, LCE, 13331 Marseille, France

Correspondence to: Joel F. de Brito (joel.brito@imt-nord-europe.fr) and Carolina Ramírez-Romero (carolina.ramirezromero@utoronto.ca)

Abstract. Volatile Organic Compounds (VOC), particularly of biogenic origin emitted by vegetation and soils, play an important role in the global Organic Aerosol (OA) budget. The introduction of field-deployable Aerosol Mass Spectrometers in the early 2000s, combined with statistical analysis of their mass spectra, has significantly improved our understanding of the impact of secondary processes on fine-mode aerosol concentrations. While delivering innovative and significant insights, those analyses usually fail to explicitly identify precursors/mechanisms. In this context, this work focuses on laboratory-generated secondary OA (SOA) of biogenic VOC and its spectral analysis through a new generation of aerosol mass spectrometers, notably a Proton Transfer Reaction Mass Spectrometer coupled to a Chemical Analysis of AeRosol Online (PTRMS-CHARON) inlet. Aerosol particles were formed in the DouAir atmospheric chamber via isoprene (ISOP) OH oxidation, monoterpene O_3 (limonene, MT), and sesquiterpene O_3 (β-caryophyllene, SQT) oxidation. ISOP experiments targeted "low-NO" environments, typically remote forested tropical areas, via epoxidiols formation (ISOP-IEPOX-SOA), or through an alternative branching favored in the absence of acidic seed particles (ISOP-Non-IEPOX-SOA) and "high NO" environments, representative in urban and polluted regions (ISOP-NO-SOA). Experiments showed that those five SOA formation pathways (ISOP-IEPOX-SOA, ISOP-Non-IEPOX-SOA, ISOP-NO-SOA, and the ozonolysis reactions of MT and SQT) exhibited distinguishable spectra, with identifiable tracer ions, such as *m/z* 83.049 (C_5H_6O), *m/z* 119.07 ($C_5H_{10}O_3$), *m/z* 137.081 ($C_5H_{12}O_4$) for ISOP-IEPOX-SOA, $C_5H_{10}O_4$ (*m/z* 135.070), $C_5H_{10}O_6$ (*m/z* 167.055) for ISOP-Non-IEPOX-SOA, and *m/z* 85.028 ($C_4H_4O_2$) for NO-SOA pathways, as well as molecules with C_7-C_{10} and C_7-C_{15} structures identified during MT and SQT oxidation experiments, respectively. These laboratory findings depict promising results for ambient near-real-time biogenic SOA source apportionment, notably in forested and/or urbanized areas.

https://doi.org/10.5194/egusphere-2025-2331
Preprint. Discussion started: 25 June 2025

1. Introduction

Globally, organic aerosol (OA) particles account for an average of ~50 % of the submicron particulate matter (PM_1, De Gouw and Jimenez, 2009), however with values ranging from 10 to 90 %, depending on the nature of the site (forested, urbanized, etc.) and atmospheric conditions (Kanakidou et al., 2005; Seinfeld and Pankow, 2003). PM largely affects radiative forcing, climate, air quality, and public health, and has therefore been the subject of intense research (Hallquist et al., 2009; Shrivastava et al., 2017; Nault et al., 2021; Pye et al., 2021). The OA fraction can originate from direct emissions, such as combustion, cooking, and biological activity, and is then referred to as primary organic aerosol (POA, Zhang et al., 2011; Heald and Spracklen, 2009). It can also be formed in the atmosphere through the oxidation of volatile organic compounds (VOC), being then referred to as secondary organic aerosol (SOA, Jimenez et al., 2009; Hallquist et al., 2009). Globally, SOA is estimated to contribute 0.88 Tg of the overall OA burden of 1.82 Tg (Hodzic et al., 2016).

The formation of SOA can undertake multiple reaction steps, where volatile precursors potentially interact with a range of oxidants such as hydroxyl radical (OH), ozone (O_3), and nitrate radical (NO_3), to form less volatile products. These can be characterized by their effective saturation concentration, C* (μg m^{-3}), into semi-volatile (SVOC, 0.3 < C* < 300 μg m^{-3}), low-volatile (LVOC, 3×10^{-4} < C* < 0.3 μg m^{-3}, and extremely low-volatile (ELVOC C* < 3×10^{-4} μg m^{-3}) organic compounds shifting their atmospheric equilibrium towards the condensed-phase (Hallquist et al., 2009; De Gouw and Jimenez, 2009; Donahue et al., 2011, 2012; Tröstl et al., 2016; Amaladhasan et al., 2022; Srivastava et al., 2022). It is currently accepted that a large fraction of SOA is formed from biogenic VOC (BVOC) precursors (Yáñez-Serrano et al., 2020; Zhang et al., 2018; Dada et al., 2023). Vegetation represents one of the most significant BVOC sources worldwide (Guenther et al., 2012). Terpenoids such as isoprene (C_5H_8), monoterpenes ($C_{10}H_{16}$), and sesquiterpenes ($C_{15}H_{24}$), are identified as the most important SOA precursors due to their emission strength and fast atmospheric reactivity (Guenther et al., 2012; Yáñez-Serrano et al., 2020). In tropical areas such as the Amazon rain forest, where remote regions still experience limited anthropogenic impact during the wet season, the atmosphere is controlled through natural processes, including SOA exclusively formed from the oxidation of BVOC (Martin et al., 2010; Andreae et al., 2015, 2018; Glicker et al., 2019; Franco et al., 2022; Leppla et al., 2025). Modeling studies in the Central Amazon have suggested that under background conditions, the SOA formation is dominated by isoprene (49 %), followed by monoterpenes (45 %, Shrivastava et al., 2019). However, recent studies reported that sesquiterpene emissions could also be of relevance to SOA formation in the Amazon (Hamilton et al., 2013; Bourtsoukidis et al., 2018). In boreal forests, for instance, monoterpenes dominate the VOC emissions and SOA formation (Hakola et al., 2012; Zhou et al., 2017; Roldin et al., 2019). Nevertheless, isoprene and sesquiterpenes can also significantly impact SOA formation in these regions (Kourtchev et al., 2008; Barreira et al., 2021; Hellén et al., 2018). In high-NO_x environments, BVOC emission has shown a relatively lower contribution to SOA formation (Ghirardo et al., 2016). Similarly, in chamber experiments, increasing NO levels perturbed isoprene-derived SOA formation, primarily due to a reduction in the contribution of non-nitrate components (D'Ambro et al., 2017). However, recent studies have highlighted that terpenoids have been shown to contribute significantly to SOA formation (Shrivastava et al., 2019; Schwantes et al., 2019).

Mass spectrometric techniques such as Aerosol Mass Spectrometers (AMS) have been extensively used in the scientific community to understand OA loadings and dynamics (Hu et al., 2015; Kristensen et al., 2017). Statistical tools such as Positive Matrix Factorization (PMF) allow for the splitting of OA into factors according to their

https://doi.org/10.5194/egusphere-2025-2331
Preprint. Discussion started: 25 June 2025

spectral signature and temporal variability (Drosatou et al., 2019). However, the high fragmentation associated with electron impact ionization hinders molecular characterization and reduces the source/process identification capabilities. In recent years, new soft ionization techniques have been implemented in mass spectrometry techniques to reduce fragmentation, allowing the identification of low-volatility compounds at the molecular level. Chemical ionization mass spectrometry (CI-MS) is one of the most common techniques considered as a soft ionization method due to the relatively low fragmentation of the analyte (Lopez-Hilfiker et al., 2014; Eichler et al., 2015). Molecular ionization is achieved by the transfer of an electron/proton/adduct of various reagent ions (e.g., Br^-, H_3O^+, NH_4^+, I^-, Huang et al., 2021).

CI-MS equipped with a H_3O^+ source (Proton-Transfer-Reaction Mass Spectrometry, PTR-MS) has been the main tool for fast and precise quantification of small organic gaseous compounds for several decades (de Gouw and Warneke, 2007). More recently, the system has been coupled with thermo-desorption (TD) aerosol inlets, termed CHemical Analysis of aeRosol ONline (CHARON-PTRMS, Eichler et al., 2015). This inlet has been used in ambient deployments (Müller et al., 2017; Piel et al., 2019; Leglise et al., 2019; Peng et al., 2023), chamber and flow reactor experiments targeting SOA formation (Gkatzelis et al., 2018a, b; Peng et al., 2023; Lannuque et al., 2023). However, a systematic study of SOA formation from BVOC oxidation using PTRMS-CHARON to explore its potential in source apportionment studies is lacking. To address this gap, we characterized the formation of SOA from biogenic precursors in the Teflon DouAir atmospheric chamber (Douai, France) employing the PTRMS-CHARON. We focused on five SOA precursors/pathways, namely monoterpene (limonene) and sesquiterpene (β-caryophyllene) ozonolysis, the isoprene-OH oxidation via the HO_2 route favoring or suppressing the epoxidiol route (IEPOX-SOA and Non-IEPOX-SOA) under low-NO conditions, and the isoprene-NO oxidation promoting the isoprene-NO-SOA in high polluted environments.

2. Materials and methods

2.1. DouAir Atmospheric Simulation Chamber

The experiments were conducted in the 9 m^3 DouAir Teflon chamber (Fig. 1), housed at IMT Nord Europe, Douai, France. This mobile chamber made of fluorinated ethylene propylene (FEP) Teflon allows the study of multiple atmospheric processes, including OH reactivity, peroxy radical chemistry, and aerosol formation, both in laboratory settings and field deployments. DouAir can be operated under dark conditions or irradiated either via natural solar light or artificial UV lamps, allowing the simulation of a wide range of atmospheric conditions. Its injection line can be heated up to 100 °C to optimize the introduction of compounds with a wide range of volatilities. The mixing time of gases is less than 4 minutes in the chamber (Supplementary Information, SI). A zero-air generator (AZ purifier 2020, Claind) coupled to a humidification system provides continuously zero air to compensate for the sampling flow rate of the analytical instruments as well as to control the relative humidity (RH), typically ranging from 8 L min^{-1} up to 40 L min^{-1}. The chamber is equipped with a large array of analytical instruments focusing on VOC, aerosol particles, and atmospheric radicals, sampling from the opposite side of the injection ports.

https://doi.org/10.5194/egusphere-2025-2331
Preprint. Discussion started: 25 June 2025

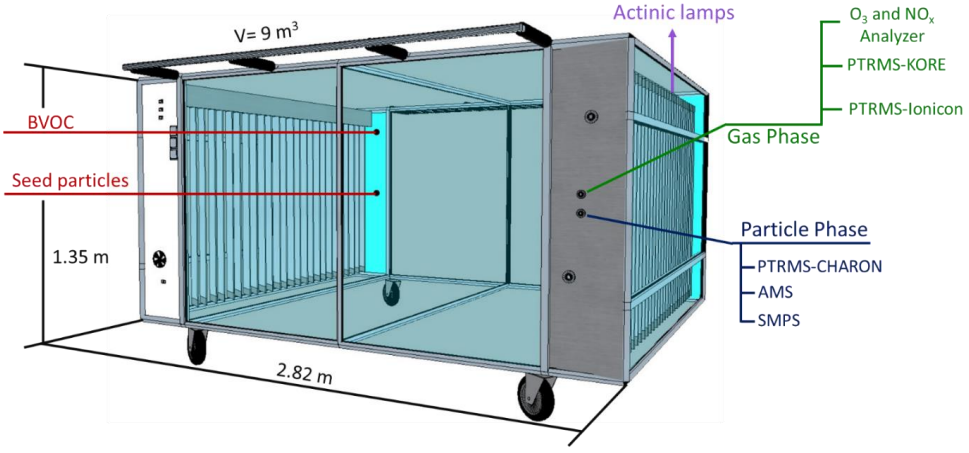

Figure 1: Schematics of the DouAir chamber depicting instrument layouts, ports, and injection points.

2.2. Instruments

The CHARON system (Ionicon Analytik Inc, Innsbruck., Austria) is an aerosol inlet for the chemical characterization of sub-micrometer particles larger than ~125 nm. The system consists of a gas-phase denuder, a critical orifice, and an aerodynamic lens (enrichment factor, EF ~21) focusing particles into a thermo-desorption unit (TDU) at 140 °C at a pressure of typically 8 mbar (Müller et al., 2014). Determination of the instrumental background is done automatically by switching the sampled air flow through a HEPA filter. CHARON has been already deployed for environmental measurements in different European cities (e.g., Lyon, Valencia, Innsbruck, Müller et al., 2017) in a rural forested site in southwest Germany (Song et al., 2023), in urban areas of East China (Peng et al., 2023) aircraft measurements over California (Piel et al., 2019) as well as in laboratory studies of SOA characterization from VOC precursors such as toluene (Lannuque et al., 2023), terpenes (Gkatzelis et al., 2018a; Gao et al., 2022), vehicle (Kostenidou et al., 2024) and tree emissions (Gkatzelis et al., 2018a, b).

The CHARON inlet is coupled here to a quadrupole interface PTRMS (PTR-QiTOF-MS; Ionicon Analytik Inc, Innsbruck, Austria; Müller et al., 2014). The pressure and temperature in the drift tube were 2.6 mbar and 80 °C, respectively. Voltages in the drift tube were set to achieve 80 Td and 100 Td for the particle and gas phase measurements, respectively. These electric fields (1Td = 10^{-17} V cm^2) determine the kinetic energy of the ions within the drift region, largely preventing the formation of water clusters but potentially leading to the fragmentation of target molecules. Lower E/N values for the particle phase were possible due to water removal by the CHARON denuder. During all experiments, the measurement time resolution was 10 s.

The gas phase calibration of the PTRMS ion transmission curve was performed using a Gas Calibration Unit (Ionicon Analytik Inc., Innsbruck, Austria) coupled to a certified gas cylinder (National Physical Laboratory; Worton et al., 2023) with RH levels comparable to the chamber experiments (15-50%). The gas cylinder contained compounds ranging up to 370 amu, including hydrocarbons (e.g., benzene, toluene, *m*-xylene) and oxygenated molecules (e.g., acetaldehyde, methyl ethyl ketone (MEK), and octamethylcyclotetrasiloxane). The quantification of particle-phase concentration requires, in addition to accurate gaseous calibration, the determination of the EF (i.e., the efficiency of particle enrichment before evaporation in the TDU and introduction into the drift tube) described in Eichler et al. (2015). The EF can be obtained by a ratio of sampling flows before and after the aerosol

https://doi.org/10.5194/egusphere-2025-2331
Preprint. Discussion started: 25 June 2025

dynamic lens or by introducing a known number of monodispersed particles as described in Eichler et al. (2015) and Peng et al. (2023). In this study, ammonium nitrate (NH_4NO_3) and levoglucosan ($C_6H_{10}O_5$) particles were used for calibration with solutions at concentrations of 0.005 M and 0.01 M, respectively. The solutions were nebulized using an atomizer (TSI 3080), and the resulting polydisperse particles were size-selected (100 nm - 400 nm) using a differential mobility analyzer (DMA; TSI 3082). The monodisperse particle size selected flow was split into the condensation particle counter (CPC; TSI 3750) and the PTRMS-CHARON. The mass concentration of particles measured by the CPC was determined assuming a shape factor of 0.8 and 1 for ammonium nitrate and levoglucosan, respectively. The ratio between CPC and PTRMS-CHARON measurements was used to derive the size-dependent EF. Levoglucosan had an estimated EF value of 24.1 ± 0.5, whereas semi-volatile NH_4NO_3 repeatedly yielded significantly lower values (~6.5 ± 1.2). It is speculated that low EF in the latter was probably linked to the evaporation of the particles inside the CHARON system. To ensure consistency across experiments, an EF value of 21 was applied, as specified by the manufacturer's certified documentation. Depending on the experimental protocol, the instrument was either operated in particle-phase sampling mode exclusively or in alternating 40 minutes particle-phase and 20 minutes gas-phase cycles.

Other mass spectrometers were used to complement PTRMS-CHARON observations, such as a second PTRMS (second generation, Kore Technology Inc.) for VOC measurements (Michoud et al., 2017). This PTRMS was operated with an E/N = 130 Td, maintaining pressures of 2.2 mbar and 1.4 mbar in the glow discharge and reactor, respectively. A VOC calibration procedure similar to PTRMS-CHARON was performed, and, for some of the experiments, a High-Resolution Aerosol Mass Spectrometer (HR-AMS, Aerodyne Research Inc.; DeCarlo et al., 2006) operated in V-mode at 30 s time resolution was coupled to the chamber. Data has been treated with the Peak Integration by Key Analysis (PIKA) module, and frequent blanks during the experiments were used to correct for fluctuations in the CO_2^+ signal at m/z 44. The HR-AMS has been calibrated using monodispersed ammonium nitrate and ammonium sulfate particles from the corresponding solutions at 0.005 M. Ancillary instrumentation consisted of a scanning mobility particle sizer (SMPS, model 3082 coupled to a butanol CPC 3750 at a range of 7 - 283 nm, TSI), an ozone monitor (POM model 202, 2B technologies), a NO_x analyzer (T200UP, Teledyne), and a RH monitor (LI-840A, Li-COR).

2.3 Experimental protocols

Three different terpenes (i.e., isoprene –ISOP; limonene, a monoterpene – MT; and β-caryophyllene, a sesquiterpene – SQT) were used as precursors for the SOA production experiments. The ISOP-SOA was formed via three main reaction pathways, known as ISOP-IEPOX-, ISOP-Non-IEPOX-, and ISOP-NO-SOA. ISOP oxidation forms isoprene-hydroxy-peroxy radicals (ISOPOO), which in turn can undergo bimolecular reactions with other organic peroxy radicals (RO_2), HO_2, or nitric oxide (NO), depending on their concentration levels, or intramolecular hydrogen shifts, notably at remote sites (Wennberg et al., 2018). Experimental conditions were designed to favor the HO_2 and NO routes, respectively. The HO_2 route led to hydroxy hydroperoxide (ISOPOOH) isomers, where the addition of significant O_3 concentrations in the chamber favored not only OH formation but also acted as a sink for NO in the chamber ($k_{OH + ISOP (298K)}$ =1.0 × 10^{-10} cm^3 $molecule^{-1}$ s^{-1}; $k_{Ozone + ISOP (298K)}$=1.27 × 10^{-17} cm^3 $molecule^{-1}$ s^{-1}; Atkinson et al., 2006). Subsequently, the addition of OH to ISOPOOH led to the formation of an alkyl radical whose fast cyclization or reaction with O_2 favors ISOP-IEPOX-SOA or ISOP-Non-IEPOX-SOA, respectively (Liu et al., 2016b). During ISOP-IEPOX and ISOP-Non-IEPOX-SOA formation, hydroxyl radical (OH) was formed via tetramethylethylene (TME, C_6H_{12}) ozonolysis, as described in detail in

https://doi.org/10.5194/egusphere-2025-2331
Preprint. Discussion started: 25 June 2025

Atkinson and Aschmann (1993), Lambe et al. (2007), and Berndt et al. (2019). On the other hand, the NO pathway favored the formation of methacryloyl peroxynitrate (MPAN), an SOA precursor, initiated by the reaction of ISOPOO radicals with NO (Surratt et al., 2010). Gas-phase products such as methyl vinyl ketone (MVK) and methacrolein (MACR) account for up to 70% (Kroll et al., 2005), thus preceding the formation of MPAN in the presence of NO. Further oxidation leads to methacrylic acid epoxide (MAE) and hydroxymethyl-methyl-a-lactone (HMML) formation (Lin et al., 2013; Nguyen et al., 2015). ISOP-NO-SOA formation was achieved through OH (formed via HONO photolysis) with seed particles and an initial concentration of NO (~8 ppb) and NO_2 (5 ppb) (Kroll et al., 2005; Surratt et al., 2010).

The enrichment of ISOP-IEPOX-SOA occurs when the acidified particles catalyze the ring-opening from the epoxide functional group, accompanied by the addition of particle-phase nucleophiles such as sulfate and water (Liu et al., 2015). This uptake reaction forms low-volatility products such as C_5-alkene triols (ca. 2-methyltetrols and $C_5H_{10}O_3$ compounds; Frauenheim et al., 2022), 4-diols, 3-methyltetrahydrofuran-3, oligomers, and organosulfates identified in ISOP-IEPOX-SOA (Kuwata et al., 2015; Liu et al., 2016a; D'Ambro et al., 2019). The ISOP-Non-IEPOX pathway (again through the HO_2 route) can form highly oxidized compounds and be an important fraction of isoprene-derived SOA (Liu et al., 2016a; Riva et al., 2016; Mettke et al., 2023). The formation of this ISOP-Non-IEPOX-SOA occurs in the absence of reactive aqueous seed particles, promoting the formation of molecules such as $C_5H_{10}O_5$, $C_5H_{12}O_5$, and $C_5H_{12}O_6$ (Liu et al., 2016a). Krechmer et al. (2015) reported that this pathway may contribute up to 3.3% of the total global SOA. The formation of ISOP-IEPOX-SOA was performed using acidic seed particles (ammonium sulfate and sulfuric acid, 0.005 M and 0.1 M, respectively) at 50% RH, whereas neutral seed particles (ammonium sulfate, 0.005M solution) at 15-30% RH were used to produce ISOP-Non-IEPOX-SOA (Surratt et al., 2010; Zhang et al., 2019; Nah et al., 2019). The method has been validated through the identification of $C_5H_6O^+$ ions in the HR-AMS following the procedure described by Hu et al. (2015). It is important to note that both ISOP-Non- and ISOP-IEPOX-SOA here correspond to "low-NO" environments, through HO_2 branching (Allan et al., 2014), and ISOP-NO-SOA to "high-NO" environments. Although the two regimes differ in SOA yields, the role of alkyl peroxy radicals (RO_2) is significant. The reaction between RO_2 and NO (representing high-NO conditions) generally results in a lower SOA yield compared to the reaction between RO_2 and HO_2 (representing low-NO conditions) (Kroll et al., 2006; Surratt et al., 2006; Xu et al., 2014). This difference is attributed to the formation of organic nitrates in high-NO environments, which are more volatile and tend to remain in the gas phase (Brégonzio-Rozier et al., 2016).

MT- and SQT-SOA were formed through the ozonolysis of limonene and β-caryophyllene, respectively, in the absence of seed particles. Both reaction pathways in terpene-derived SOA formation have been well understood and extensively studied in Teflon chambers (Zhang et al., 2006; Chen et al., 2012; Kundu et al., 2017; Tasoglou and Pandis, 2015; Gkatzelis et al., 2018b, a). The details of the chamber experiments are given in Table 1. For all experiments, humidification of the chamber was the initiating step to allow background measurements by all instruments. For ISOP-Non and ISOP-IEPOX-SOA experiments, seed particles and O_3 were injected before the isoprene injection. The TME injections were conducted every 5 minutes for approximately 4 hours in order to keep a significant production of OH all along the experiments. During ISOP-IEPOX-SOA experiments, continuous injection of seed particles was performed to ensure the presence of acidic particles in the chamber.

https://doi.org/10.5194/egusphere-2025-2331
Preprint. Discussion started: 25 June 2025

Similarly to the ISOP experiments, ozone was injected before the MT and SQT injections. Four injections of limonene were performed at intervals of 20 min for MT-SOA experiments, and six injections of β-caryophyllene at intervals between 20 and 45 min for SQT-SOA experiments. Sequential injections of MT and SQT were performed to avoid nucleation events and promote condensation and reactive uptake of semi-volatile compounds on the particles already present from the first injection. The experiments were done at 15-50 % RH and room temperature (air-conditioned room at ~20 °C). After each experiment, DouAir was flushed continuously with purified air for at least 24 hours at a flow rate of 40 L min^{-1}. All the measurements were corrected for dilution and wall losses as detailed in the SI.

Table 1. Summary of experimental conditions during the chamber experiments.

Experiment (# of repetitions)	Seed particles	Injection of biogenic precursor in ppbv (# of injections)	Ozone (ppb)	Injection of TME in ppbv (# of injections)	OH (molecules cm^{-3})	Maximun SOA formed (μgm^{-3})	SOA formation conditions
ISOP-IEPOX-SOA (3)	$(NH_4)_2SO_4$+H_2SO_4	200 (1)	80-100	10 (27)	~4 x 10^5	~5	Reaction with OH
ISOP-Non-IEPOX SOA (2)	$(NH_4)_2SO_4$	100 (2)	80-100	10 (19)	~4 x 10^5	~4	Reaction with OH
ISOP-NO-SOA (1)	$(NH_4)_2SO_4$	90 (1)	~100		~4 x 10^6	~3	Reaction with OH
MT-SOA (5)	----	18 (3)	80 initial		----	~120	Ozonolysis
SQT-SOA (3)	----	10 (6)	100 initial		----	~83	Ozonolysis

3. Results and discussion

The concentration of gas and particulate species during the BSOA formation experiments are shown in Figure 2. For the ISOP experiments, the time t = 0 refers to the first injection of the seed particles, while for MT and SQT, it refers to the first injection of the biogenic precursor. Fig. 2 shows the concentration of VOC precursors, namely isoprene (*m/z* 69.07), limonene (*m/z* 81.07 and *m/z* 137.131), and β-caryophyllene (*m/z* 81.070, 95.086, 109.101, 123.117, 135.117, 137.131, 149.132, and 205.195; Kim et al., 2009). The precursor gas concentration peaked at ~190 ppb, ~220 ppb, ~90 ppb for ISOP-IEPOX-, ISOP-Non-IEPOX-, and ISOP-NO-SOA experiments respectively, ~40 ppb for MT (injections totaling 72 ppb), whereas maximum SQT concentration has been roughly 5 ppb for a total injected of 60 ppb, due to its high reactivity. In the ISOP-NO-SOA experiment, peak of ~300 ppb isoprene was observed at first detection, stabilizing to 90 ppb for 2 min, ensuring proper mixing in the chamber. The large difference between the total MT and SQT injected levels and those observed in the chamber is associated with the high reactivity of MT and SQT with O_3, leading to fast consumption once injected in the chamber. Additional factors that may contribute to these differences include losses on the chamber walls and inside the PTRMS inlet.

The first-oxidation products of the biogenic precursors are also shown in Fig. 2. For ISOP, the depicted compounds are methyl-vinyl ketone (MVK, C_4H_6O), methacrolein (MACR, C_4H_6O), and ISOPOOH ($C_5H_{10}O_3$), their sum being detected at *m/z* 71.049 (Liu et al., 2013; Bernhammer et al., 2017). The oxidation products of MT shown here are levulinic acid ($C_5H_8O_3$, *m/z* 117.055 + *m/z* 99.044), limonalic acid, norlimononic acid, and ketolimononaldehyde ($C_9H_{14}O_3$, *m/z* 171.102 + *m/z* 153.091) (Gkatzelis et al., 2018a, b). The selected SQT oxidation products were β-caryophyllinic acid ($C_{14}H_{22}O_4$, *m/z* 255.159 + *m/z* 237.149), β-caryophyllene aldehyde ($C_{15}H_{24}O_2$, *m/z* 237.185 + *m/z* 219.174) and β-caryophyllonic acid ($C_{15}H_{24}O_3$, *m/z* 253.180 + *m/z* 235.169) (Li et al., 2011; Chan et al., 2011; Gao et al., 2022).

https://doi.org/10.5194/egusphere-2025-2331
Preprint. Discussion started: 25 June 2025

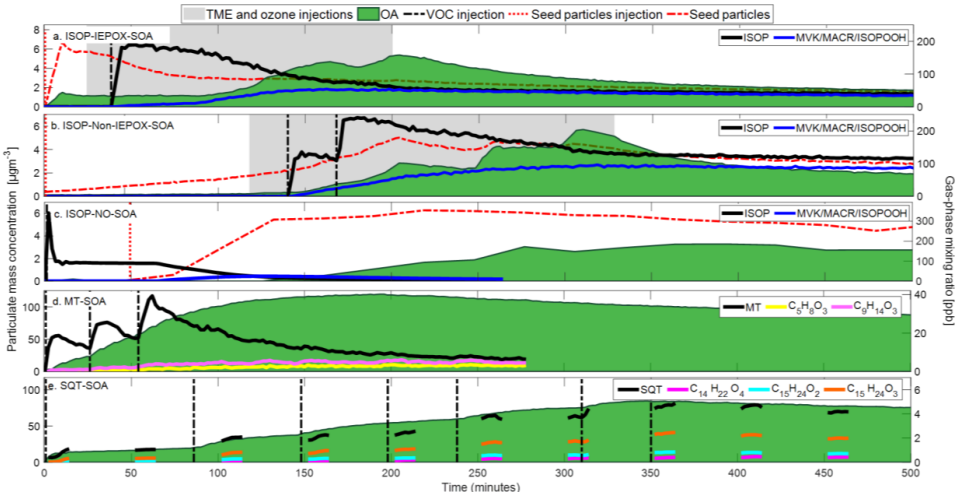

Figure 2: Concentration of particulate and gaseous species during the following experiments: (a) ISOP-IEPOX-SOA, (b) ISOP-Non-IEPOX-SOA, (c) ISOP-NO-SOA, (d) MT-SOA, and (e) SQT-SOA. Seed particles are shown in red, SOA in green, and the gaseous precursors in cyan whereas oxidation products in the gas-phase have different colors for different experiments. The vertical red and cyan dashed lines represent the injection of seed particles and VOC precursors, respectively, and the grey areas correspond to OH production via O_3 + TME injections. The seed particle signal was divided by 4 and 2 for ISOP-IEPOX and ISOP-Non-IEPOX-SOA experiments, respectively, for better visualization. The SQT mixing ratios in panel d have been calculated as the sum of *m/z* 81.070, 95.086, 109.101, 123.117, 135.117, 137.131, 149.132, and 205.195. Measurements of gas precursors in the SQT experiments are discontinuous due to the switching between gas and particle phase measurements in the PTRMS-CHARON.

The HR-AMS has also been used to distinguish ISOP-IEPOX and ISOP-Non-IEPOX-SOA routes, namely through the use of the ratio of C_5H_6O to the total OA signal (termed $f_{C_5H_6O}$, Hu et al., 2015). This signal (or its unit mass resolution ion in AMS, *m/z* 82) was first reported by Robinson et al. (2011) in the Borneo Forest, under high isoprene conditions. Subsequently, Lin et al. (2012) confirmed that the signal corresponds to methyl furan, a thermal decomposition product of cis- and trans-3-methyltetrahydrofuran-3,4-diols (3-MeTHF-3,4-diols), a product of the reactive uptake of IEPOX. Methyl furan has also been observed in the Central Amazon (de Sá et al., 2018; Schulz et al., 2018), Southeastern USA (Liao et al., 2015; Xu et al., 2015b, a), and Canada (Slowik et al., 2011), among other environments. The f_{CO_2} (or in unit mass resolution f_{44}) can be associated with OA oxidation level and aging degree of OA (Cubison et al., 2011; Milic et al., 2017; Morgan et al., 2020)

Figure 3 compares f_{CO_2} and $f_{C_5H_6O}$ from the ISOP experiments, as well as chamber results from the literature associated with ISOP-IEPOX-SOA (Lin et al., 2012; Budisulistiorini et al., 2013; Canagaratna et al., 2015; Kuwata et al., 2015; Liu et al., 2015). The results indicate that the protocol applied here, mainly associated with seed particle acidity and RH, successfully separated IEPOX and non-IEPOX oxidations for the experiments, albeit having both low-NO conditions.

https://doi.org/10.5194/egusphere-2025-2331
Preprint. Discussion started: 25 June 2025

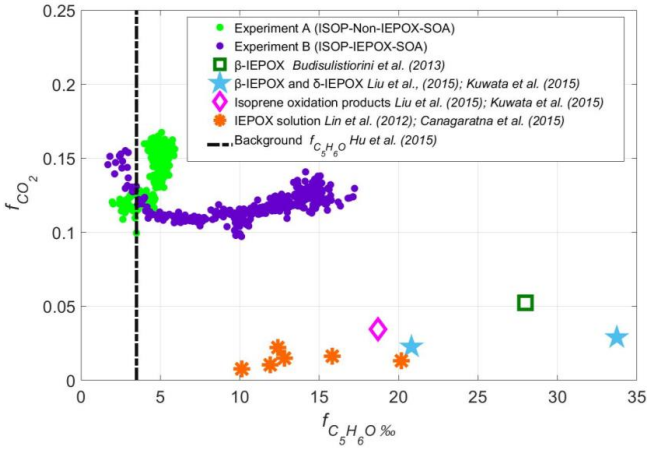

Figure 3: Scatter plot of f_{CO_2} vs $f_{C_5H_6O}$ for the ISOP-SOA experiments conducted in the DouAir atmospheric chamber. Successful production of IEPOX-SOA has been obtained by increasing the RH (20% to 50%) and having acidic seed particles. The figure also includes laboratory experiments of whether IEPOX uptake or isoprene oxidation.

Figure 4 shows the time series of the aerosol concentration on ISOP-IEPOX-SOA experiment, as well as CHARON observations of *m/z* 119.07 ($C_5H_{10}O_3$) and *m/z* 137.081 ($C_5H_{12}O_4$) referred to as "C5-alkene triols", previously reported in the literature as tracers of ISOP-IEPOX-SOA (Frauenheim et al., 2022; Lopez-Hilfiker et al., 2016; D'Ambro et al., 2019). In addition, it is interesting to note the *m/z* 83.049 (C_5H_6O) detected in PTRMS-CHARON also has a high signal, suggesting a similar process of IEPOX-SOA identification as through Aerosol Mass Spectrometry (Hu et al., 2015).

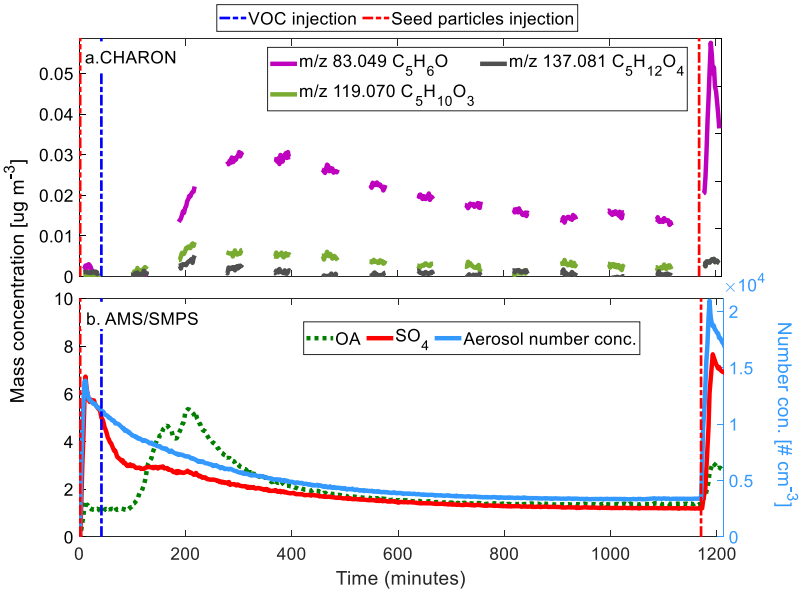

https://doi.org/10.5194/egusphere-2025-2331
Preprint. Discussion started: 25 June 2025

Figure 4: Time series of (a) selected ions detected by PTRMS-CHARON during the ISOP-IEPOX-SOA experiment and (b) mass (left axis) and number (right axis) aerosol concentrations measured by AMS and SMPS, respectively. The measurements in panel (a) are discontinuous due to the switching between gas and particle phases in the PTRMS-CHARON.

Figure 5 depicts the signature spectrum for the experiments studied here. For ISOP-Non-IEPOX-, MT-, and SQT-SOA, the signature spectra were chosen for the period when OA peaked. For ISOP-IEPOX-SOA, strongly dependent on seed particle acidity, the chosen period corresponds to the second acidic seed particle injection, after gas-phase oxidation was underway, when the highest measured C_5H_6O by the CHARON. Panel a depicts the fingerprint for ISOP-IEPOX-SOA, notably dominated by C_5H_6O, $C_2H_4O_3$ (*m/z* 77.023), $C_5H_8O_4$ (*m/z* 133.05), and $C_9H_{12}O_3$ (*m/z* 169.086). Mettke et al. (2023) showed that $C_5H_8O_4$ is a product of the uptake of ISOPOOH, and this molecule was also found in the formation of SOA from standardized isomers of ISOPOOH and isoprene oxidation (Krechmer et al., 2015; D'Ambro et al., 2017). The ion associated with $C_5H_8O_2$ (*m/z* 101.060) was also observed here and can be associated with the fragmentation of $C_5H_{10}O_3$ (shown in Fig. 4) through a dehydration process.

Generally, the average spectrum of ISOP-Non-IEPOX-SOA (Fig. 5b) also depicts major contributions from C_5 compounds, with some overlapping ions such as $C_5H_8O_2$, $C_5H_8O_4$, $C_5H_6O_2$ (*m/z* 99.044), and $C_5H_8O_3$ (*m/z* 117.055), but differing relative contributions. The latter, more strongly identified in the ISOP-Non-IEPOX-SOA pathway, might be a fragment of $C_5H_{10}O_4$ (*m/z* 135.070), identified in the literature as a marker of ISOP-Non-IEPOX-SOA (Mettke et al., 2023). Similarly, $C_5H_8O_2$ may be enhanced via fragmentation of $C_5H_{10}O_3$ (*m/z* 119.07), although the latter was not observed here. $C_5H_{10}O_6$ (*m/z* 167.055), a known product of the reactive uptake of ISOPOOH in the ISOP-Non-IEPOX-SOA pathway, was identified here (Liu et al., 2016b; Mettke et al., 2023). $C_5H_{10}O_5$, $C_5H_{12}O_5$, and $C_5H_{12}O_6$, also cited in the literature, however, were not observed during those experiments. It is important to note that CHARON also detects C_5H_6O at the ISOP-Non-IEPOX-SOA route, contrary to HR-AMS. Caution is warranted when using this ion as a tracer for epoxydiol-derived SOA in PTRMS-CHARON measurements, and a comprehensive evaluation through a combined chamber and field studies is necessary to confirm the robustness of this tracer.

Figure 5c shows that the spectrum of ISOP-NO-SOA is predominantly characterized by C_4 compounds, including $C_4H_4O_{2\text{-}3}$ (*m/z* 85.028; *m/z* 101.023), $C_4H_6O_{1\text{-}2}$ (*m/z* 71.049; *m/z* 87.044), and $C_4H_8O_{1\text{-}2}$ (*m/z* 73.065; *m/z* 89.060). The compound $C_4H_4O_2$, a fragment of $C_4H_6O_3$, has been previously reported in studies of ISOP-NO_x irradiation (Jia and Xu, 2018) and methacrolein (MACR)-NO_x irradiation (Lin et al., 2013). The mass ion $C_4H_6O_3$ has been identified as a fundamental unit in the oligomerization of 2-methylglyceric acid (2-MGA) in SOA formation, where it serves as a molecular tracer for ISOP-SOA (Kleindienst et al., 2007; Nguyen et al., 2011; Zhang et al., 2011a). Among the C_5 compounds, $C_5H_6O_{1\text{-}2}$ (*m/z* 83.049; *m/z* 99.044), C_5H_8O (*m/z* 85.065) was detected, whereas C_5H_6O and C_5H_8O had been identified in ISOP-SOA under low-NO conditions. Their identification could be attributed to the low yield of ISOP-SOA during isoprene hydroxy nitrates formation (Jacobs et al., 2014). The mass ion $C_6H_8O_4$ (*m/z* 145.050) has similarly been identified by Schwantes et al. (2019), which was shown to result from the esterification of 2-MGA with acids in the particle phase (Chan et al., 2010). Mass ions $C_3H_4O_2$ (*m/z* 73.028), and $C_3H_6O_2$ (*m/z* 75.044) were detected at high intensities, with the latter previously identified as hydroxyacetone (Jia and Xu, 2018).

https://doi.org/10.5194/egusphere-2025-2331
Preprint. Discussion started: 25 June 2025

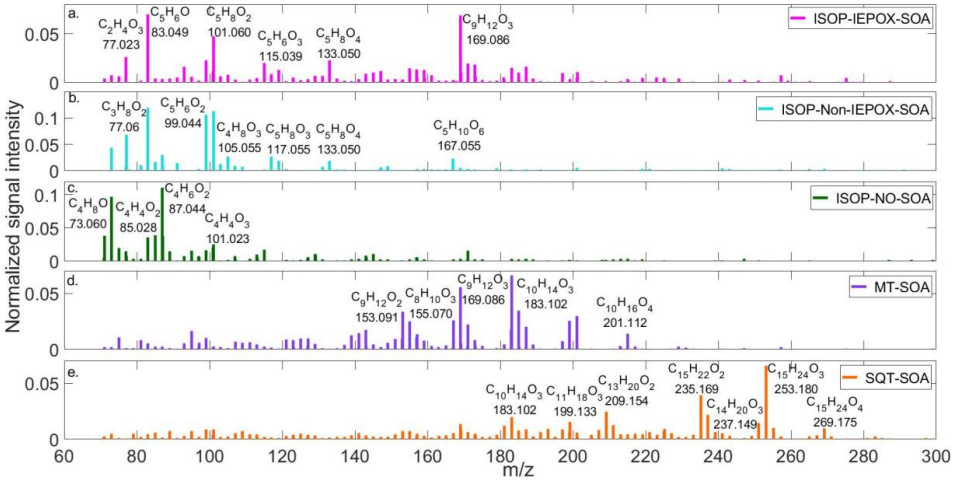

Figure 5: Signature spectra of (a) ISOP-IEPOX-SOA, (b) ISOP-Non-IEPOX-SOA, (c) MT-SOA, (d) SQT-SOA as detected by PTRMS-CHARON.

Similar to the ISOP-SOA experiments, the contribution of compounds for MT- and SQT-SOA is distributed between main ions and likely fragments, some of which were previously reported by the literature. Using PTRM-CHARON, Gkatzelis et al. (2018a) reported highly oxidized semi-volatile compounds during limonene ozonolysis such as $C_9H_{14}O_3$ (*m/z* 171.102), $C_8H_{12}O_4$ (*m/z* 173.081), $C_{10}H_{16}O_3$ (*m/z* 185.117), $C_9H_{14}O_4$ (*m/z* 187.096), $C_8H_{12}O_5$ (*m/z* 189.075) and $C_{10}H_{16}O_4$ (*m/z* 201.112) and their potential fragments, *m/z* 153.091 ($C_9H_{12}O_2$), *m/z* 155.070 ($C_8H_{10}O_3$), *m/z* 167.106 ($C_{10}H_{14}O_2$), *m/z* 169.086 ($C_9H_{12}O_3$), *m/z* 171.065 ($C_8H_{10}O_4$) and *m/z* 183.102 ($C_{10}H_{14}O_3$), which were also identified in MT-SOA experiments in the DouAir chamber. $C_9H_{12}O_4$ (*m/z* 185.081), a potential fragment of $C_9H_{14}O_5$ (*m/z* 203.091), was also identified and previously reported by Jacob et al. (2023) using Liquid Chromatography Mass Spectrometry (LC-MS). During SQT-SOA experiments main ions such as *m/z* 237.185 ($C_{15}H_{24}O_2$), 239.164 ($C_{14}H_{22}O_3$), *m/z* 253.180 ($C_{15}H_{24}O_3$), *m/z* 255.159 ($C_{14}H_{22}O_4$), *m/z* 269.175 ($C_{15}H_{24}O_4$), *m/z* 271.190 ($C_{15}H_{26}O_4$), and their fragments *m/z* 219.174 ($C_{15}H_{22}O$), *m/z* 221.154 ($C_{14}H_{20}O_2$), *m/z* 235.169 ($C_{15}H_{22}O_2$), *m/z* 237.149 ($C_{14}H_{20}O_3$), *m/z* 251.164 ($C_{15}H_{22}O_3$), *m/z* 253.180 ($C_{15}H_{24}O_3$) were identified. These signals were previously reported by Gao et al. (2022), identifying them with PTRMS-CHARON at different temperatures during the ozonolysis of β-caryophyllene. The ion on *m/z* 199.133 ($C_{11}H_{18}O_3$), corresponding to an oxidation product of β-caryophyllene called 3,3-dimethyl-2-(3-oxobutyl) cyclobutane carboxylic acid, was also found during the SQT experiments (Li et al., 2011; Jaoui et al., 2013).

https://doi.org/10.5194/egusphere-2025-2331
Preprint. Discussion started: 25 June 2025

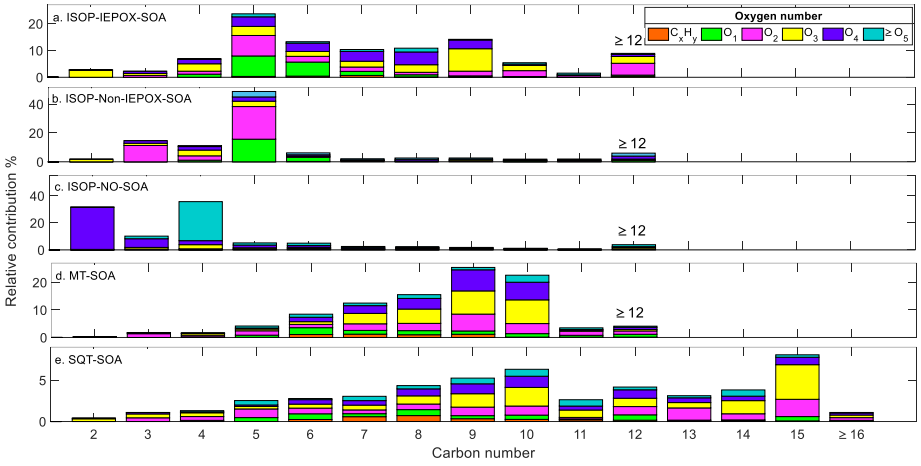

Figure 6: Relative contributions of the total OA fraction for (a) ISOP-EPOX-SOA, (b) ISOP-Non-IEPOX-SOA, (c) MT-SOA, and (d) SQT-SOA. The SOA fraction distribution is based on the number of carbons and oxygens in the detected ions.

The different SOA spectra obtained with PTRMS-CHARON have been studied according to their number of carbons and oxygens, as shown in Fig. 6. Following the results presented previously, ions associated with C_5 molecules/fragments dominated both ISOP-SOA pathways under low-NO_x conditions, being responsible for roughly ~50% and ~25% contribution in ISOP-Non-IEPOX- and ISOP-IEPOX-SOA, respectively. The contribution of C_5 compounds in the Non-IEPOX-SOA route is comparable to that reported by Liu et al. (2016a) using a FIGAERO HF-ToF-CIMS (52 %). D'Ambro et al. (2017) also observed the same behavior, attributing ~64% of the OA to C_5 compounds during the first hours of isoprene oxidation. On the other hand, C_4 molecules dominated the ISOP-NO-SOA experiment with ~35% of the total OA mass, followed by ~31% of C_2 molecules. The prominent C_2-C_4 molecules identified in this experiment share the same molecular skeletons as species reported in similar studies by Jia and Xu (2018).

Non-sulfated dimers and low volatile oligomers have been evidenced in the formation of IEPOX-SOA in laboratory studies (Surratt et al., 2006; Lin et al., 2014; Armstrong et al., 2022). Surratt et al. (2006) and Lin et al. (2014) reported the presence of dimers (e.g., $C_{10}H_{22}O_7$ and $C_{10}H_{20}O_6$) during the laboratory experiments. Armstrong et al. (2022) also suggested that the decomposition of non-sulfated oligomers is possible in the presence of OH, which leads to lower molecular weight compounds with low volatility. The presence of oligomers, and their subsequent decomposition, in addition to the fragmentation already known in PTRMS-CHARON may explain the distribution of the SOA fraction measured in this work, which is more diverse than during the previously described ISOP-Non-IEPOX-SOA route.

The varied distribution of molecules in the mass fraction was also evident in MT- and SQT-SOA. MT-SOA shows a mass fraction is distributed between C_7-C_{10} molecules as also reported by Gkatzelis et al. (2018a). Its major contribution is attributed mainly to C_9 and C_{10} ions, reaching up to 48%, with C_7-C_9 ions accounting for about ~37%. Oxygenated molecules (O_3-O_4) comprise most of the SOA mass detected by PTRMS-CHARON.

https://doi.org/10.5194/egusphere-2025-2331
Preprint. Discussion started: 25 June 2025

The distribution of the detected ions is more homogeneous than the distribution seen in Non-IEPOX-SOA, which may be influenced by a degree of fragmentation of larger molecules. This same behavior was also identified in the SQT-SOA where its contribution is more evenly distributed as a function of carbon number. The highest contribution is in C_{15} molecules followed by C_7-C_9 and C_{14}. Highly oxygenated compounds were also important in the fraction of SOA. The O_3-O_4 molecules contribute ~50 % of the SOA fraction during β-caryophyllene ozonolysis.

4. Conclusions

This study presents, for the first time, a systematic characterization of BSOA using PTRMS-CHARON. Building on a platform widely used worldwide for gas-phase VOC measurements, the CHARON module extends its application to particulate-phase compounds, an area of growing interest. The experiments, conducted at the DouAir atmospheric simulation chamber, investigated SOA formation from five distinct pathways: three isoprene-related mechanisms: ISOP-IEPOX-SOA, ISOP-Non-IEPOX-SOA, and ISOP-NO-SOA. The first two are representative of low-NO chemistry, whereas the latter is of high-NO. Two terpenoid-derived pathways were also studied, MT-SOA (monoterpenes) and SQT-SOA (sesquiterpenes).

The isoprene chamber experiments yielded SOA mass loadings from 3-5 μg m^{-3}, whereas MT and SQT were in the tens of 80-120 μg m^{-3}. Results showed a distinct chemical fingerprint with a distribution on mass loadings and specific ions for each of the formation pathways that can assist in field observations and factor analysis. During the ISOP-IEPOX-SOA experiment, well known tracers were identified (e.g., *m/z* 119.07 ($C_5H_{10}O_3$) and *m/z* 137.081 ($C_5H_{12}O_4$)). In parallel, $C_5H_{10}O_4$ (*m/z* 135.070) and *m/z* 167.055 ($C_5H_{10}O_6$) have been identified in the ISOP-Non-IEPOX-SOA pathway. It is important to note that several ions, including C_5H_6O, a well-known tracer for ISOP-IEPOX using aerosol mass spectrometry, were identified in both low-NO ISOP-SOA experiments, and thus, care must be taken when interpreting field observations. The high-NO experiment could identify tracers of 2-MGA, such as *m/z* 85.028 ($C_4H_4O_2$), alongside other molecules.

The limonene and β-caryophyllene ozonolysis were used for the study of MT- and SQT-SOA, respectively. In these experiments, C_7-C_{10} and C_{11}-C_{15} molecules were identified. A relevant contribution of potential fragments $[M+H-H_2O]^+$ of characteristic ions previously reported was also evidenced, which shows the importance of the characterization of fragments in these types of methods.

This study provides a systematic experimental framework for investigating SOA formation. When applied to PTRMS-CHARON, it delivers reference spectra that enhance source identification under varying NO conditions and across multiple BVOC precursors. By characterizing both main ions and their fragments, this work advances the interpretation of complex ambient mixtures and improves the reliability of SOA source attribution. In the context of the diverse analytical tools available for studying semi-volatile species, such targeted studies are essential for refining and complementing existing methodologies. The insights gained here may serve as a valuable guide for identifying reaction pathways and supporting ambient measurements using PTRMS-CHARON.

Author contributions. CRR, OM, and JFB designed the chamber experiments. CRR, OM, HB, LF, and MJ carried out experiments and supervised the laboratory work. JFB, CP, and SS supervised the scientific work. CRR and OM analysed the data. CRR wrote the manuscript with contributions from all coauthors.

https://doi.org/10.5194/egusphere-2025-2331
Preprint. Discussion started: 25 June 2025

Competing interests. The contact author has declared that none of the authors has any competing interests.

Acknowledgments

IMT Nord Europe acknowledges financial support from CPER ECRIN project funded by the Regional Council "Hauts-de-France", the European Regional Development Fund (ERDF), CaPPA, and AREA. The CaPPA project (Chemical and Physical Properties of the Atmosphere) is funded by the French National Research Agency (ANR) through the PIA (Programme d'Investissement d'Avenir) under contract "ANR-11-LABX-0005-01". The French State under the France-2030 programme and the Initiative of Excellence of the University of Lille are acknowledged for the funding and support granted to the R-CDP-24-003-AREA project. Max Planck Institute for Chemistry acknowledges financial support from the Max Planck Society and the Bundesministerium für Bildung und Forschung (BMBF contract 01LK2101B).

Financial support. This work was supported by the Regional Council "Hauts-de-France," ERDF, CaPPA (ANR-11-LABX-0005-01), AREA (R-CDP-24-003), the Max Planck Society, and BMBF (01LK2101B).

References

Allan, J. D., Morgan, W. T., Darbyshire, E., Flynn, M. J., Williams, P. I., Oram, D. E., Artaxo, P., Brito, J., Lee, J. D., and Coe, H.: Airborne observations of IEPOX-derived isoprene SOA in the Amazon during SAMBBA, Atmos. Chem. Phys., 14, 11393–11407, https://doi.org/10.5194/acp-14-11393-2014, 2014.

Amaladhasan, D. A., Heyn, C., Hoyle, C. R., El Haddad, I., Elser, M., Pieber, S. M., Slowik, J. G., Amorim, A., Duplissy, J., Ehrhart, S., Makhmutov, V., Molteni, U., Rissanen, M., Stozhkov, Y., Wagner, R., Hansel, A., Kirkby, J., Donahue, N. M., Volkamer, R., Baltensperger, U., Gysel-Beer, M., and Zuend, A.: Modelling the gas--particle partitioning and water uptake of isoprene-derived secondary organic aerosol at high and low relative humidity, Atmos. Chem. Phys., 22, 215–244, https://doi.org/10.5194/acp-22-215-2022, 2022.

Andreae, M. O., Acevedo, O. C., Araùjo, A., Artaxo, P., Barbosa, C. G. G., Barbosa, H. M. J., Brito, J., Carbone, S., Chi, X., Cintra, B. B. L., da Silva, N. F., Dias, N. L., Dias-Júnior, C. Q., Ditas, F., Ditz, R., Godoi, A. F. L., Godoi, R. H. M., Heimann, M., Hoffmann, T., Kesselmeier, J., Könemann, T., Krüger, M. L., Lavric, J. V, Manzi, A. O., Lopes, A. P., Martins, D. L., Mikhailov, E. F., Moran-Zuloaga, D., Nelson, B. W., Nölscher, A. C., Santos Nogueira, D., Piedade, M. T. F., Pöhlker, C., Pöschl, U., Quesada, C. A., Rizzo, L. V, Ro, C.-U., Ruckteschler, N., Sá, L. D. A., de Oliveira Sá, M., Sales, C. B., dos Santos, R. M. N., Saturno, J., Schöngart, J., Sörgel, M., de Souza, C. M., de Souza, R. A. F., Su, H., Targhetta, N., Tóta, J., Trebs, I., Trumbore, S., van Eijck, A., Walter, D., Wang, Z., Weber, B., Williams, J., Winderlich, J., Wittmann, F., Wolff, S., and Yáñez-Serrano, A. M.: The Amazon Tall Tower Observatory (ATTO): overview of pilot measurements on ecosystem ecology, meteorology, trace gases, and aerosols, Atmos. Chem. Phys., 15, 10723–10776, https://doi.org/10.5194/acp-15-10723-2015, 2015.

Andreae, M. O., Afchine, A., Albrecht, R., Holanda, B. A., Artaxo, P., Barbosa, H. M. J., Borrmann, S., Cecchini, M. A., Costa, A., Dollner, M., Fütterer, D., Järvinen, E., Jurkat, T., Klimach, T., Konemann, T., Knote, C., Krämer, M., Krisna, T., Machado, L. A. T., Mertes, S., Minikin, A., Pöhlker, C., Pöhlker, M. L., Pöschl, U.,

https://doi.org/10.5194/egusphere-2025-2331
Preprint. Discussion started: 25 June 2025

Rosenfeld, D., Sauer, D., Schlager, H., Schnaiter, M., Schneider, J., Schulz, C., Spanu, A., Sperling, V. B., Voigt, C., Walser, A., Wang, J., Weinzierl, B., Wendisch, M., and Ziereis, H.: Aerosol characteristics and particle production in the upper troposphere over the Amazon Basin, Atmos. Chem. Phys., 18, 921–961, https://doi.org/10.5194/acp-18-921-2018, 2018.

Armstrong, N. C., Chen, Y., Cui, T., Zhang, Y., Christensen, C., Zhang, Z., Turpin, B. J., Chan, M. N., Gold, A., Ault, A. P., and Surratt, J. D.: Isoprene epoxydiol-derived sulfated and nonsulfated oligomers suppress particulate mass loss during oxidative aging of secondary organic aerosol, Environ. Sci. Technol., 56, 16611–16620, https://doi.org/10.1021/acs.est.2c03200, 2022.

Atkinson, R. and Aschmann, S. M.: Hydroxyl radical production from the gas-phase reactions of ozone with a series of alkenes under atmospheric conditions, Environ. Sci. Technol., 27, 1357–1363, https://doi.org/10.1021/es00044a010, 1993.

Atkinson, R., Baulch, D. L., Cox, R. A., Crowley, J. N., Hampson, R. F., Hynes, R. G., Jenkin, M. E., Rossi, M. J., Troe, J., and IUPAC Subcommittee: Evaluated kinetic and photochemical data for atmospheric chemistry: Volume II - gas phase reactions of organic species, Atmos. Chem. Phys., 6, 3625–4055, https://doi.org/10.5194/acp-6-3625-2006, 2006.

Barreira, L. M. F., Ylisirniö, A., Pullinen, I., Buchholz, A., Li, Z., Lipp, H., Junninen, H., Hõrrak, U., Noe, S. M., Krasnova, A., Krasnov, D., Kask, K., Talts, E., Niinemets, Ü., Ruiz-Jimenez, J., and Schobesberger, S.: The importance of sesquiterpene oxidation products for secondary organic aerosol formation in a springtime hemiboreal forest, Atmos. Chem. Phys., 21, 11781–11800, https://doi.org/10.5194/acp-21-11781-2021, 2021.

Berndt, T., Hyttinen, N., Herrmann, H., and Hansel, A.: First oxidation products from the reaction of hydroxyl radicals with isoprene for pristine environmental conditions, Commun. Chem., 2, 21, https://doi.org/10.1038/s42004-019-0120-9, 2019.

Bernhammer, A.-K., Breitenlechner, M., Keutsch, F. N., and Hansel, A.: Technical note: Conversion of isoprene hydroxy hydroperoxides (ISOPOOHs) on metal environmental simulation chamber walls, Atmos. Chem. Phys., 17, 4053–4062, https://doi.org/10.5194/acp-17-4053-2017, 2017.

Bourtsoukidis, E., Behrendt, T., Yañez-Serrano, A. M., Hellén, H., Diamantopoulos, E., Catão, E., Ashworth, K., Pozzer, A., Quesada, C. A., Martins, D. L., Sá, M., Araujo, A., Brito, J., Artaxo, P., Kesselmeier, J., Lelieveld, J., and Williams, J.: Strong sesquiterpene emissions from Amazonian soils, Nat. Commun., 9, 2226, https://doi.org/10.1038/s41467-018-04658-y, 2018.

Brégonzio-Rozier, L., Giorio, C., Siekmann, F., Pangui, E., Morales, S. B., Temime-Roussel, B., Gratien, A., Michoud, V., Cazaunau, M., DeWitt, H. L., Tapparo, A., Monod, A., and Doussin, J.-F.: Secondary organic aerosol formation from isoprene photooxidation during cloud condensation-evaporation cycles, Atmos. Chem. Phys., 16, 1747–1760, https://doi.org/10.5194/acp-16-1747-2016, 2016.

https://doi.org/10.5194/egusphere-2025-2331
Preprint. Discussion started: 25 June 2025

Budisulistiorini, S. H., Canagaratna, M. R., Croteau, P. L., Marth, W. J., Baumann, K., Edgerton, E. S., Shaw, S. L., Knipping, E. M., Worsnop, D. R., Jayne, J. T., Gold, A., and Surratt, J. D.: Real-Time Continuous Characterization of Secondary Organic Aerosol Derived from Isoprene Epoxydiols in Downtown Atlanta, Georgia, Using the Aerodyne Aerosol Chemical Speciation Monitor, Environ. Sci. Technol., 47, 5686–5694, https://doi.org/10.1021/es400023n, 2013.

Canagaratna, M. R., Jimenez, J. L., Kroll, J. H., Chen, Q., Kessler, S. H., Massoli, P., Hildebrandt Ruiz, L., Fortner, E., Williams, L. R., Wilson, K. R., Surratt, J. D., Donahue, N. M., Jayne, J. T., and Worsnop, D. R.: Elemental ratio measurements of organic compounds using aerosol mass spectrometry: characterization, improved calibration, and implications, Atmos. Chem. Phys., 15, 253–272, https://doi.org/10.5194/acp-15-253-2015, 2015.

Chan, A. W. H., Chan, M. N., Surratt, J. D., Chhabra, P. S., Loza, C. L., Crounse, J. D., Yee, L. D., Flagan, R. C., Wennberg, P. O., and Seinfeld, J. H.: Role of aldehyde chemistry and NO_x concentrations in secondary organic aerosol formation, Atmos. Chem. Phys., 10, 7169–7188, https://doi.org/10.5194/acp-10-7169-2010, 2010.

Chan, M. N., Surratt, J. D., Chan, A. W. H., Schilling, K., Offenberg, J. H., Lewandowski, M., Edney, E. O., Kleindienst, T. E., Jaoui, M., Edgerton, E. S., Tanner, R. L., Shaw, S. L., Zheng, M., Knipping, E. M., and Seinfeld, J. H.: Influence of aerosol acidity on the chemical composition of secondary organic aerosol from β-caryophyllene, Atmos. Chem. Phys., 11, 1735–1751, https://doi.org/10.5194/acp-11-1735-2011, 2011.

Chen, Q., Li, Y. L., McKinney, K. A., Kuwata, M., and Martin, S. T.: Particle mass yield from β-caryophyllene ozonolysis, Atmos. Chem. Phys., 12, 3165–3179, https://doi.org/10.5194/acp-12-3165-2012, 2012.

Cubison, M. J., Ortega, A. M., Hayes, P. L., Farmer, D. K., Day, D., Lechner, M. J., Brune, W. H., Apel, E., Diskin, G. S., Fisher, J. A., Fuelberg, H. E., Hecobian, A., Knapp, D. J., Mikoviny, T., Riemer, D., Sachse, G. W., Sessions, W., Weber, R. J., Weinheimer, A. J., Wisthaler, A., and Jimenez, J. L.: Effects of aging on organic aerosol from open biomass burning smoke in aircraft and laboratory studies, Atmos. Chem. Phys., 11, 12049–12064, https://doi.org/10.5194/acp-11-12049-2011, 2011.

D'Ambro, E. L., Lee, B. H., Liu, J., Shilling, J. E., Gaston, C. J., Lopez-Hilfiker, F. D., Schobesberger, S., Zaveri, R. A., Mohr, C., Lutz, A., Zhang, Z., Gold, A., Surratt, J. D., Rivera-Rios, J. C., Keutsch, F. N., and Thornton, J. A.: Molecular composition and volatility of isoprene photochemical oxidation secondary organic aerosol under low- and high-NO_x conditions, Atmos. Chem. Phys., 17, 159–174, https://doi.org/10.5194/acp-17-159-2017, 2017.

D'Ambro, E. L., Schobesberger, S., Gaston, C. J., Lopez-Hilfiker, F. D., Lee, B. H., Liu, J., Zelenyuk, A., Bell, D., Cappa, C. D., Helgestad, T., Li, Z., Guenther, A., Wang, J., Wise, M., Caylor, R., Surratt, J. D., Riedel, T., Hyttinen, N., Salo, V.-T., Hasan, G., Kurtén, T., Shilling, J. E., and Thornton, J. A.: Chamber-based insights into the factors controlling epoxydiol (IEPOX) secondary organic aerosol (SOA) yield, composition, and volatility, Atmos. Chem. Phys., 19, 11253–11265, https://doi.org/10.5194/acp-19-11253-2019, 2019.

https://doi.org/10.5194/egusphere-2025-2331
Preprint. Discussion started: 25 June 2025

Dada, L., Stolzenburg, D., Simon, M., Fischer, L., Heinritzi, M., Wang, M., Xiao, M., Vogel, A. L., Ahonen, L., Amorim, A., Baalbaki, R., Baccarini, A., Baltensperger, U., Bianchi, F., Daellenbach, K. R., DeVivo, J., Dias, A., Dommen, J., Duplissy, J., Finkenzeller, H., Hansel, A., He, X.-C., Hofbauer, V., Hoyle, C. R., Kangasluoma, J., Kim, C., Kürten, A., Kvashnin, A., Mauldin, R., Makhmutov, V., Marten, R., Mentler, B., Nie, W., Petäjä, T., Quéléver, L. L. J., Saathoff, H., Tauber, C., Tome, A., Molteni, U., Volkamer, R., Wagner, R., Wagner, A. C., Wimmer, D., Winkler, P. M., Yan, C., Zha, Q., Rissanen, M., Gordon, H., Curtius, J., Worsnop, D. R., Lehtipalo, K., Donahue, N. M., Kirkby, J., Haddad, I. El, and Kulmala, M.: Role of sesquiterpenes in biogenic new particle formation, Sci. Adv., 9, eadi5297, https://doi.org/10.1126/sciadv.adi5297, 2023.

DeCarlo, P. F., Kimmel, J. R., Trimborn, A., Northway, M. J., Jayne, J. T., Aiken, A. C., Gonin, M., Fuhrer, K., Horvath, T., Docherty, K. S., Worsnop, D. R., and Jimenez, J. L.: Field-deployable, high-resolution, time-of-flight aerosol mass spectrometer., Anal. Chem., 78, 8281–8289, https://doi.org/10.1021/ac061249n, 2006.

Donahue, N. M., Epstein, S. A., Pandis, S. N., and Robinson, A. L.: A two-dimensional volatility basis set: 1. organic-aerosol mixing thermodynamics, Atmos. Chem. Phys., 11, 3303–3318, https://doi.org/10.5194/acp-11-3303-2011, 2011.

Donahue, N. M., Kroll, J. H., Pandis, S. N., and Robinson, A. L.: A two-dimensional volatility basis set – Part 2: Diagnostics of organic-aerosol evolution, Atmos. Chem. Phys., 12, 615–634, https://doi.org/10.5194/acp-12-615-2012, 2012.

Drosatou, A. D., Skyllakou, K., Theodoritsi, G. N., and Pandis, S. N.: Positive matrix factorization of organic aerosol: insights from a chemical transport model, Atmos. Chem. Phys., 19, 973–986, https://doi.org/10.5194/acp-19-973-2019, 2019.

Eichler, P., Müller, M., D'Anna, B., and Wisthaler, A.: A novel inlet system for online chemical analysis of semi-volatile submicron particulate matter, Atmos. Meas. Tech., 8, 1353–1360, https://doi.org/10.5194/amt-8-1353-2015, 2015.

Franco, M. A., Ditas, F., Kremper, L. A., Machado, L. A. T., Andreae, M. O., Araújo, A., Barbosa, H. M. J., de Brito, J. F., Carbone, S., Holanda, B. A., Morais, F. G., Nascimento, J. P., Pöhlker, M. L., Rizzo, L. V, Sá, M., Saturno, J., Walter, D., Wolff, S., Pöschl, U., Artaxo, P., and Pöhlker, C.: Occurrence and growth of sub-50 nm aerosol particles in the Amazonian boundary layer, Atmos. Chem. Phys., 22, 3469–3492, https://doi.org/10.5194/acp-22-3469-2022, 2022.

Frauenheim, M., Offenberg, J., Zhang, Z., Surratt, J. D., and Gold, A.: The C_5–Alkene Triol Conundrum: Structural Characterization and Quantitation of Isoprene-Derived $C_5H_{10}O_3$ Reactive Uptake Products, Environ. Sci. Technol. Lett., 9, 829–836, https://doi.org/10.1021/acs.estlett.2c00548, 2022.

Gao, L., Song, J., Mohr, C., Huang, W., Vallon, M., Jiang, F., Leisner, T., and Saathoff, H.: Kinetics, SOA yields, and chemical composition of secondary organic aerosol from β-caryophyllene ozonolysis with and without nitrogen oxides between 213 and 313 K, Atmos. Chem. Phys., 22, 6001–6020, https://doi.org/10.5194/acp-22-

https://doi.org/10.5194/egusphere-2025-2331
Preprint. Discussion started: 25 June 2025

6001-2022, 2022.

Ghirardo, A., Xie, J., Zheng, X., Wang, Y., Grote, R., Block, K., Wildt, J., Mentel, T., Kiendler-Scharr, A., Hallquist, M., Butterbach-Bahl, K., and Schnitzler, J.-P.: Urban stress-induced biogenic VOC emissions and SOA-forming potentials in Beijing, Atmos. Chem. Phys., 16, 2901–2920, https://doi.org/10.5194/acp-16-2901-2016, 2016.

Gkatzelis, G. I., Tillmann, R., Hohaus, T., Müller, M., Eichler, P., Xu, K.-M., Schlag, P., Schmitt, S. H., Wegener, R., Kaminski, M., Holzinger, R., Wisthaler, A., and Kiendler-Scharr, A.: Comparison of three aerosol chemical characterization techniques utilizing PTR-ToF-MS: a study on freshly formed and aged biogenic SOA, Atmos. Meas. Tech., 11, 1481–1500, https://doi.org/10.5194/amt-11-1481-2018, 2018a.

Gkatzelis, G. I., Hohaus, T., Tillmann, R., Gensch, I., Müller, M., Eichler, P., Xu, K.-M., Schlag, P., Schmitt, S. H., Yu, Z., Wegener, R., Kaminski, M., Holzinger, R., Wisthaler, A., and Kiendler-Scharr, A.: Gas-to-particle partitioning of major biogenic oxidation products: a study on freshly formed and aged biogenic SOA, Atmos. Chem. Phys., 18, 12969–12989, https://doi.org/10.5194/acp-18-12969-2018, 2018b.

Glicker, H. S., Lawler, M. J., Ortega, J., de Sá, S. S., Martin, S. T., Artaxo, P., Vega Bustillos, O., de Souza, R., Tota, J., Carlton, A., and Smith, J. N.: Chemical composition of ultrafine aerosol particles in central Amazonia during the wet season, Atmos. Chem. Phys., 19, 13053–13066, https://doi.org/10.5194/acp-19-13053-2019, 2019.

de Gouw, J. and Warneke, C.: Measurements of volatile organic compounds in the earth's atmosphere using proton-transfer-reaction mass spectrometry, Mass Spectrom. Rev., 26, 223–257, https://doi.org/https://doi.org/10.1002/mas.20119, 2007.

de Gouw, J. and Jimenez, J. L.: Organic Aerosols in the Earth's Atmosphere, Environ. Sci. Technol., 43, 7614–7618, https://doi.org/10.1021/es9006004, 2009.

Guenther, A. B., Jiang, X., Heald, C. L., Sakulyanontvittaya, T., Duhl, T., Emmons, L. K., and Wang, X.: The Model of Emissions of Gases and Aerosols from Nature version 2.1 (MEGAN2.1): an extended and updated framework for modeling biogenic emissions, Geosci. Model Dev., 5, 1471–1492, https://doi.org/10.5194/gmd-5-1471-2012, 2012.

Hakola, H., Hellén, H., Hemmilä, M., Rinne, J., and Kulmala, M.: In situ measurements of volatile organic compounds in a boreal forest, Atmos. Chem. Phys., 12, 11665–11678, https://doi.org/10.5194/acp-12-11665-2012, 2012.

Hallquist, M., Wenger, J. C., Baltensperger, U., Rudich, Y., Simpson, D., Claeys, M., Dommen, J., Donahue, N. M., George, C., Goldstein, A. H., Hamilton, J. F., Herrmann, H., Hoffmann, T., Iinuma, Y., Jang, M., Jenkin, M. E., Jimenez, J. L., Kiendler-Scharr, A., Maenhaut, W., McFiggans, G., Mentel, T. F., Monod, A., Prévôt, A. S. H., Seinfeld, J. H., Surratt, J. D., Szmigielski, R., and Wildt, J.: The formation, properties and impact of secondary organic aerosol: current and emerging issues, Atmos. Chem. Phys., 9, 5155–5236,

https://doi.org/10.5194/egusphere-2025-2331
Preprint. Discussion started: 25 June 2025

https://doi.org/10.5194/acp-9-5155-2009, 2009.

Hamilton, J. F., Alfarra, M. R., Robinson, N., Ward, M. W., Lewis, A. C., McFiggans, G. B., Coe, H., and Allan, J. D.: Linking biogenic hydrocarbons to biogenic aerosol in the Borneo rainforest, Atmos. Chem. Phys., 13, 11295–11305, https://doi.org/10.5194/acp-13-11295-2013, 2013.

Heald, C. L. and Spracklen, D. V.: Atmospheric budget of primary biological aerosol particles from fungal spores, Geophys. Res. Lett., 36, https://doi.org/https://doi.org/10.1029/2009GL037493, 2009.

Hellén, H., Praplan, A. P., Tykkä, T., Ylivinkka, I., Vakkari, V., Bäck, J., Petäjä, T., Kulmala, M., and Hakola, H.: Long-term measurements of volatile organic compounds highlight the importance of sesquiterpenes for the atmospheric chemistry of a boreal forest, Atmos. Chem. Phys., 18, 13839–13863, https://doi.org/10.5194/acp-18-13839-2018, 2018.

Hodzic, A., Kasibhatla, P. S., Jo, D. S., Cappa, C. D., Jimenez, J. L., Madronich, S., and Park, R. J.: Rethinking the global secondary organic aerosol (SOA) budget: stronger production, faster removal, shorter lifetime, Atmos. Chem. Phys., 16, 7917–7941, https://doi.org/10.5194/acp-16-7917-2016, 2016.

Hu, W. W., Campuzano-Jost, P., Palm, B. B., Day, D. A., Ortega, A. M., Hayes, P. L., Krechmer, J. E., Chen, Q., Kuwata, M., Liu, Y. J., de Sá, S. S., McKinney, K., Martin, S. T., Hu, M., Budisulistiorini, S. H., Riva, M., Surratt, J. D., St. Clair, J. M., Isaacman-Van Wertz, G., Yee, L. D., Goldstein, A. H., Carbone, S., Brito, J., Artaxo, P., de Gouw, J. A., Koss, A., Wisthaler, A., Mikoviny, T., Karl, T., Kaser, L., Jud, W., Hansel, A., Docherty, K. S., Alexander, M. L., Robinson, N. H., Coe, H., Allan, J. D., Canagaratna, M. R., Paulot, F., and Jimenez, J. L.: Characterization of a real-time tracer for isoprene epoxydiols-derived secondary organic aerosol (IEPOX-SOA) from aerosol mass spectrometer measurements, Atmos. Chem. Phys., 15, 11807–11833, https://doi.org/10.5194/acp-15-11807-2015, 2015.

Huang, W., Li, H., Sarnela, N., Heikkinen, L., Tham, Y. J., Mikkilä, J., Thomas, S. J., Donahue, N. M., Kulmala, M., and Bianchi, F.: Measurement report: Molecular composition and volatility of gaseous organic compounds in a boreal forest - from volatile organic compounds to highly oxygenated organic molecules, Atmos. Chem. Phys., 21, 8961–8977, https://doi.org/10.5194/acp-21-8961-2021, 2021.

Jacob, F., Houzel, N., Genevray, P., Clety, C., Coeur, C., Perdrix, E., Alleman, L. Y., Anthérieu, S., Garçon, G., Dhont, G., Cuisset, A., Lo Guidice, J.-M., and Tomas, A.: New insights into the chemical composition and formation mechanisms of secondary organic aerosols produced in the ozonolysis of limonene, J. Aerosol Sci., 173, 106214, https://doi.org/https://doi.org/10.1016/j.jaerosci.2023.106214, 2023.

Jacobs, M. I., Burke, W. J., and Elrod, M. J.: Kinetics of the reactions of isoprene-derived hydroxynitrates: gas phase epoxide formation and solution phase hydrolysis, Atmos. Chem. Phys., 14, 8933–8946, https://doi.org/10.5194/acp-14-8933-2014, 2014.

Jaoui, M., Kleindienst, T. E., Docherty, K. S., Lewandowski, M., and Offenberg, J. H.: Secondary organic

https://doi.org/10.5194/egusphere-2025-2331
Preprint. Discussion started: 25 June 2025

aerosol formation from the oxidation of a series of sesquiterpenes: α-cedrene, β-caryophyllene, α-humulene and α-farnesene with O_3, OH and NO_3 radicals, Environ. Chem., 10, 178–193, 2013.

Jia, L. and Xu, Y.: Different roles of water in secondary organic aerosol formation from toluene and isoprene, Atmos. Chem. Phys., 18, 8137–8154, https://doi.org/10.5194/acp-18-8137-2018, 2018.

Jimenez, J. L., Canagaratna, M. R., Donahue, N. M., Prevot, A. S. H., Zhang, Q., Kroll, J. H., DeCarlo, P. F., Allan, J. D., Coe, H., Ng, N. L., Aiken, A. C., Docherty, K. S., Ulbrich, I. M., Grieshop, A. P., Robinson, A. L., Duplissy, J., Smith, J. D., Wilson, K. R., Lanz, V. A., Hueglin, C., Sun, Y. L., Tian, J., Laaksonen, A., Raatikainen, T., Rautiainen, J., Vaattovaara, P., Ehn, M., Kulmala, M., Tomlinson, J. M., Collins, D. R., Cubison, M. J., E., Dunlea, J., Huffman, J. A., Onasch, T. B., Alfarra, M. R., Williams, P. I., Bower, K., Kondo, Y., Schneider, J., Drewnick, F., Borrmann, S., Weimer, S., Demerjian, K., Salcedo, D., Cottrell, L., Griffin, R., Takami, A., Miyoshi, T., Hatakeyama, S., Shimono, A., Sun, J. Y., Zhang, Y. M., Dzepina, K., Kimmel, J. R., Sueper, D., Jayne, J. T., Herndon, S. C., Trimborn, A. M., Williams, L. R., Wood, E. C., Middlebrook, A. M., Kolb, C. E., Baltensperger, U., and Worsnop, D. R.: Evolution of Organic Aerosols in the Atmosphere, Science., 326, 1525–1529, https://doi.org/10.1126/science.1180353, 2009.

Kanakidou, M., Seinfeld, J. H., Pandis, S. N., Barnes, I., Dentener, F. J., Facchini, M. C., Van Dingenen, R., Ervens, B., Nenes, A., Nielsen, C. J., Swietlicki, E., Putaud, J. P., Balkanski, Y., Fuzzi, S., Horth, J., Moortgat, G. K., Winterhalter, R., Myhre, C. E. L., Tsigaridis, K., Vignati, E., Stephanou, E. G., and Wilson, J.: Organic aerosol and global climate modelling: a review, Atmos. Chem. Phys., 5, 1053–1123, https://doi.org/10.5194/acp-5-1053-2005, 2005.

Kim, S., Karl, T., Helmig, D., Daly, R., Rasmussen, R., and Guenther, A.: Measurement of atmospheric sesquiterpenes by proton transfer reaction-mass spectrometry (PTR-MS), Atmos. Meas. Tech., 2, 99–112, https://doi.org/10.5194/amt-2-99-2009, 2009.

Kleindienst, T. E., Jaoui, M., Lewandowski, M., Offenberg, J. H., Lewis, C. W., Bhave, P. V., and Edney, E. O.: Estimates of the contributions of biogenic and anthropogenic hydrocarbons to secondary organic aerosol at a southeastern US location, Atmos. Environ., 41, 8288–8300, https://doi.org/https://doi.org/10.1016/j.atmosenv.2007.06.045, 2007.

Kostenidou, E., Marques, B., Temime-Roussel, B., Liu, Y., Vansevenant, B., Sartelet, K., and D'Anna, B.: Secondary organic aerosol formed by Euro 5 gasoline vehicle emissions: chemical composition and gas-to-particle phase partitioning, Atmos. Chem. Phys., 24, 2705–2729, https://doi.org/10.5194/acp-24-2705-2024, 2024.

Kourtchev, I., Ruuskanen, T. M., Keronen, P., Sogacheva, L., Dal Maso, M., Reissell, A., Chi, X., Vermeylen, R., Kulmala, M., Maenhaut, W., and Claeys, M.: Determination of isoprene and α-/β-pinene oxidation products in boreal forest aerosols from Hyytiälä, Finland: diel variations and possible link with particle formation events, Plant Biol., 10, 138–149, https://doi.org/https://doi.org/10.1055/s-2007-964945, 2008.

Krechmer, J. E., Coggon, M. M., Massoli, P., Nguyen, T. B., Crounse, J. D., Hu, W., Day, D. A., Tyndall, G.

https://doi.org/10.5194/egusphere-2025-2331
Preprint. Discussion started: 25 June 2025

S., Henze, D. K., Rivera-Rios, J. C., Nowak, J. B., Kimmel, J. R., Mauldin, R. L. I. I. I., Stark, H., Jayne, J. T., Sipilä, M., Junninen, H., St. Clair, J. M., Zhang, X., Feiner, P. A., Zhang, L., Miller, D. O., Brune, W. H., Keutsch, F. N., Wennberg, P. O., Seinfeld, J. H., Worsnop, D. R., Jimenez, J. L., and Canagaratna, M. R.: Formation of Low Volatility Organic Compounds and Secondary Organic Aerosol from Isoprene Hydroxyhydroperoxide Low-NO Oxidation, Environ. Sci. Technol., 49, 10330–10339, https://doi.org/10.1021/acs.est.5b02031, 2015.

Kristensen, K., Jensen, L. N., Glasius, M., and Bilde, M.: The effect of sub-zero temperature on the formation and composition of secondary organic aerosol from ozonolysis of alpha-pinene, Environ. Sci. Process. Impacts, 19, 1220–1234, https://doi.org/10.1039/C7EM00231A, 2017.

Kroll, J. H., Ng, N. L., Murphy, S. M., Flagan, R. C., and Seinfeld, J. H.: Secondary organic aerosol formation from isoprene photooxidation under high-NO_x conditions, Geophys. Res. Lett., 32, L18808, https://doi.org/https://doi.org/10.1029/2005GL023637, 2005.

Kroll, J. H., Ng, N. L., Murphy, S. M., Flagan, R. C., and Seinfeld, J. H.: Secondary Organic Aerosol Formation from Isoprene Photooxidation, Environ. Sci. Technol., 40, 1869–1877, https://doi.org/10.1021/es0524301, 2006.

Kundu, S., Fisseha, R., Putman, A. L., Rahn, T. A., and Mazzoleni, L. R.: Molecular formula composition of β-caryophyllene ozonolysis SOA formed in humid and dry conditions, Atmos. Environ., 154, 70–81, https://doi.org/https://doi.org/10.1016/j.atmosenv.2016.12.031, 2017.

Kuwata, M., Liu, Y., McKinney, K., and Martin, S. T.: Physical state and acidity of inorganic sulfate can regulate the production of secondary organic material from isoprene photooxidation products, Phys. Chem. Chem. Phys., 17, 5670–5678, https://doi.org/10.1039/C4CP04942J, 2015.

Lambe, A. T., Zhang, J., Sage, A. M., and Donahue, N. M.: Controlled OH Radical Production via Ozone-Alkene Reactions for Use in Aerosol Aging Studies, Environ. Sci. Technol., 41, 2357–2363, https://doi.org/10.1021/es061878e, 2007.

Lannuque, V., D'Anna, B., Kostenidou, E., Couvidat, F., Martinez-Valiente, A., Eichler, P., Wisthaler, A., Müller, M., Temime-Roussel, B., Valorso, R., and Sartelet, K.: Gas-particle partitioning of toluene oxidation products: an experimental and modeling study, Atmos. Chem. Phys., 23, 15537–15560, https://doi.org/10.5194/acp-23-15537-2023, 2023.

Leglise, J., Müller, M., Piel, F., Otto, T., and Wisthaler, A.: Bulk Organic Aerosol Analysis by Proton-Transfer-Reaction Mass Spectrometry: An Improved Methodology for the Determination of Total Organic Mass, O:C and H:C Elemental Ratios, and the Average Molecular Formula, Anal. Chem., 91, 12619–12624, https://doi.org/10.1021/acs.analchem.9b02949, 2019.

Leppla, D., Hildmann, S., Zannoni, N., Kremper, L., Hollanda, B., Williams, J., Pöhlker, C., Wolff, S., Sà, M., Solci, M. C., Pöschl, U., and Hoffmann, T.: Comprehensive Non-targeted Molecular Characterization of

https://doi.org/10.5194/egusphere-2025-2331
Preprint. Discussion started: 25 June 2025

Organic Aerosols in the Amazon Rainforest, EGUsphere [preprint], https://doi.org/10.5194/egusphere-2025-141, 2025.

Li, Y. J., Chen, Q., Guzman, M. I., Chan, C. K., and Martin, S. T.: Second-generation products contribute substantially to the particle-phase organic material produced by β-caryophyllene ozonolysis, Atmos. Chem. Phys., 11, 121–132, https://doi.org/10.5194/acp-11-121-2011, 2011.

Liao, J., Froyd, K. D., Murphy, D. M., Keutsch, F. N., Yu, G., Wennberg, P. O., St. Clair, J. M., Crounse, J. D., Wisthaler, A., Mikoviny, T., Jimenez, J. L., Campuzano-Jost, P., Day, D. A., Hu, W., Ryerson, T. B., Pollack, I. B., Peischl, J., Anderson, B. E., Ziemba, L. D., Blake, D. R., Meinardi, S., and Diskin, G.: Airborne measurements of organosulfates over the continental U.S., J. Geophys. Res. Atmos., 120, 2990–3005, https://doi.org/https://doi.org/10.1002/2014JD022378, 2015.

Lin, Y.-H., Zhang, Z., Docherty, K. S., Zhang, H., Budisulistiorini, S. H., Rubitschun, C. L., Shaw, S. L., Knipping, E. M., Edgerton, E. S., Kleindienst, T. E., Gold, A., and Surratt, J. D.: Isoprene Epoxydiols as Precursors to Secondary Organic Aerosol Formation: Acid-Catalyzed Reactive Uptake Studies with Authentic Compounds, Environ. Sci. Technol., 46, 250–258, https://doi.org/10.1021/es202554c, 2012.

Lin, Y.-H., Zhang, H., Pye, H. O. T., Zhang, Z., Marth, W. J., Park, S., Arashiro, M., Cui, T., Budisulistiorini, S. H., Sexton, K. G., Vizuete, W., Xie, Y., Luecken, D. J., Piletic, I. R., Edney, E. O., Bartolotti, L. J., Gold, A., and Surratt, J. D.: Epoxide as a precursor to secondary organic aerosol formation from isoprene photooxidation in the presence of nitrogen oxides, Proc. Natl. Acad. Sci. USA, 110, 6718–6723, https://doi.org/10.1073/pnas.1221150110, 2013.

Lin, Y.-H., Budisulistiorini, S. H., Chu, K., Siejack, R. A., Zhang, H., Riva, M., Zhang, Z., Gold, A., Kautzman, K. E., and Surratt, J. D.: Light-Absorbing Oligomer Formation in Secondary Organic Aerosol from Reactive Uptake of Isoprene Epoxydiols, Environ. Sci. Technol., 48, 12012–12021, https://doi.org/10.1021/es503142b, 2014.

Liu, J., D'Ambro, E. L., Lee, B. H., Lopez-Hilfiker, F. D., Zaveri, R. A., Rivera-Rios, J. C., Keutsch, F. N., Iyer, S., Kurten, T., Zhang, Z., Gold, A., Surratt, J. D., Shilling, J. E., and Thornton, J. A.: Efficient Isoprene Secondary Organic Aerosol Formation from a Non-IEPOX Pathway, Environ. Sci. Technol., 50, 9872–9880, https://doi.org/10.1021/acs.est.6b01872, 2016a.

Liu, Y., Kuwata, M., Strick, B. F., Geiger, F. M., Thomson, R. J., McKinney, K. A., and Martin, S. T.: Uptake of Epoxydiol Isomers Accounts for Half of the Particle-Phase Material Produced from Isoprene Photooxidation via the HO2 Pathway, Environ. Sci. Technol., 49, 250–258, https://doi.org/10.1021/es5034298, 2015.

Liu, Y., Brito, J., Dorris, M. R., Rivera-Rios, J. C., Seco, R., Bates, K. H., Artaxo, P., Duvoisin, S., Keutsch, F. N., Kim, S., Goldstein, A. H., Guenther, A. B., Manzi, A. O., Souza, R. A. F., Springston, S. R., Watson, T. B., McKinney, K. A., and Martin, S. T.: Isoprene photochemistry over the Amazon rainforest, Proc. Natl. Acad. Sci., 113, 6125–6130, https://doi.org/10.1073/pnas.1524136113, 2016.

https://doi.org/10.5194/egusphere-2025-2331
Preprint. Discussion started: 25 June 2025

Liu, Y. J., Herdlinger-Blatt, I., McKinney, K. A., and Martin, S. T.: Production of methyl vinyl ketone and methacrolein via the hydroperoxyl pathway of isoprene oxidation, Atmos. Chem. Phys., 13, 5715–5730, https://doi.org/10.5194/acp-13-5715-2013, 2013.

Lopez-Hilfiker, F. D., Mohr, C., Ehn, M., Rubach, F., Kleist, E., Wildt, J., Mentel, T. F., Lutz, A., Hallquist, M., Worsnop, D., and Thornton, J. A.: A novel method for online analysis of gas and particle composition: description and evaluation of a Filter Inlet for Gases and AEROsols (FIGAERO), Atmos. Meas. Tech., 7, 983–1001, https://doi.org/10.5194/amt-7-983-2014, 2014.

Lopez-Hilfiker, F. D., Mohr, C., D'Ambro, E. L., Lutz, A., Riedel, T. P., Gaston, C. J., Iyer, S., Zhang, Z., Gold, A., Surratt, J. D., Lee, B. H., Kurten, T., Hu, W. W., Jimenez, J., Hallquist, M., and Thornton, J. A.: Molecular Composition and Volatility of Organic Aerosol in the Southeastern U.S.: Implications for IEPOX Derived SOA, Environ. Sci. Technol., 50, 2200–2209, https://doi.org/10.1021/acs.est.5b04769, 2016.

Martin, S. T., Andreae, M. O., Artaxo, P., Baumgardner, D., Chen, Q., Goldstein, A. H., Guenther, A., Heald, C. L., Mayol-Bracero, O. L., McMurry, P. H., Pauliquevis, T., Pöschl, U., Prather, K. A., Roberts, G. C., Saleska, S. R., Silva Dias, M. A., Spracklen, D. V, Swietlicki, E., and Trebs, I.: Sources and properties of Amazonian aerosol particles, Rev. Geophys., 48, RG2002, https://doi.org/https://doi.org/10.1029/2008RG000280, 2010.

Mettke, P., Brüggemann, M., Mutzel, A., Gräfe, R., and Herrmann, H.: Secondary Organic Aerosol (SOA) through Uptake of Isoprene Hydroxy Hydroperoxides (ISOPOOH) and its Oxidation Products, ACS Earth Sp. Chem., 7, 1025–1037, https://doi.org/10.1021/acsearthspacechem.2c00385, 2023.

Michoud, V., Sciare, J., Sauvage, S., Dusanter, S., Léonardis, T., Gros, V., Kalogridis, C., Zannoni, N., Féron, A., Petit, J.-E., Crenn, V., Baisnée, D., Sarda-Estève, R., Bonnaire, N., Marchand, N., DeWitt, H. L., Pey, J., Colomb, A., Gheusi, F., Szidat, S., Stavroulas, I., Borbon, A., and Locoge, N.: Organic carbon at a remote site of the western Mediterranean Basin: sources and chemistry during the ChArMEx SOP2 field experiment, Atmos. Chem. Phys., 17, 8837–8865, https://doi.org/10.5194/acp-17-8837-2017, 2017.

Milic, A., Mallet, M. D., Cravigan, L. T., Alroe, J., Ristovski, Z. D., Selleck, P., Lawson, S. J., Ward, J., Desservettaz, M. J., Paton-Walsh, C., Williams, L. R., Keywood, M. D., and Miljevic, B.: Biomass burning and biogenic aerosols in northern Australia during the SAFIRED campaign, Atmos. Chem. Phys., 17, 3945–3961, https://doi.org/10.5194/acp-17-3945-2017, 2017.

Morgan, W. T., Allan, J. D., Bauguitte, S., Darbyshire, E., Flynn, M. J., Lee, J., Liu, D., Johnson, B., Haywood, J., Longo, K. M., Artaxo, P. E., and Coe, H.: Transformation and ageing of biomass burning carbonaceous aerosol over tropical South America from aircraft in situ measurements during SAMBBA, Atmos. Chem. Phys., 20, 5309–5326, https://doi.org/10.5194/acp-20-5309-2020, 2020.

Müller, M., Mikoviny, T., Feil, S., Haidacher, S., Hanel, G., Hartungen, E., Jordan, A., Märk, L., Mutschlechner, P., Schottkowsky, R., Sulzer, P., Crawford, J. H., and Wisthaler, A.: A compact PTR-ToF-MS instrument for airborne measurements of volatile organic compounds at high spatiotemporal resolution, Atmos.

https://doi.org/10.5194/egusphere-2025-2331
Preprint. Discussion started: 25 June 2025

Meas. Tech., 7, 3763–3772, https://doi.org/10.5194/amt-7-3763-2014, 2014.

Müller, M., Eichler, P., D'Anna, B., Tan, W., and Wisthaler, A.: Direct Sampling and Analysis of Atmospheric Particulate Organic Matter by Proton-Transfer-Reaction Mass Spectrometry, Anal. Chem., 89, 10889–10897, https://doi.org/10.1021/acs.analchem.7b02582, 2017.

Nah, T., Xu, L., Osborne-Benthaus, K. A., White, S. M., France, S., and Ng, N. L.: Mixing order of sulfate aerosols and isoprene epoxydiols affects secondary organic aerosol formation in chamber experiments, Atmos. Environ., 217, 116953, https://doi.org/https://doi.org/10.1016/j.atmosenv.2019.116953, 2019.

Nault, B. A., Jo, D. S., McDonald, B. C., Campuzano-Jost, P., Day, D. A., Hu, W., Schroder, J. C., Allan, J., Blake, D. R., Canagaratna, M. R., Coe, H., Coggon, M. M., DeCarlo, P. F., Diskin, G. S., Dunmore, R., Flocke, F., Fried, A., Gilman, J. B., Gkatzelis, G., Hamilton, J. F., Hanisco, T. F., Hayes, P. L., Henze, D. K., Hodzic, A., Hopkins, J., Hu, M., Huey, L. G., Jobson, B. T., Kuster, W. C., Lewis, A., Li, M., Liao, J., Nawaz, M. O., Pollack, I. B., Peischl, J., Rappenglück, B., Reeves, C. E., Richter, D., Roberts, J. M., Ryerson, T. B., Shao, M., Sommers, J. M., Walega, J., Warneke, C., Weibring, P., Wolfe, G. M., Young, D. E., Yuan, B., Zhang, Q., de Gouw, J. A., and Jimenez, J. L.: Secondary organic aerosols from anthropogenic volatile organic compounds contribute substantially to air pollution mortality, Atmos. Chem. Phys., 21, 11201–11224, https://doi.org/10.5194/acp-21-11201-2021, 2021.

Nguyen, T. B., Roach, P. J., Laskin, J., Laskin, A., and Nizkorodov, S. A.: Effect of humidity on the composition of isoprene photooxidation secondary organic aerosol, Atmos. Chem. Phys., 11, 6931–6944, https://doi.org/10.5194/acp-11-6931-2011, 2011.

Nguyen, T. B., Bates, K. H., Crounse, J. D., Schwantes, R. H., Zhang, X., Kjaergaard, H. G., Surratt, J. D., Lin, P., Laskin, A., Seinfeld, J. H., and Wennberg, P. O.: Mechanism of the hydroxyl radical oxidation of methacryloyl peroxynitrate (MPAN) and its pathway toward secondary organic aerosol formation in the atmosphere, Phys. Chem. Chem. Phys., 17, 17914–17926, https://doi.org/10.1039/C5CP02001H, 2015.

Peng, Y., Wang, H., Gao, Y., Jing, S., Zhu, S., Huang, D., Hao, P., Lou, S., Cheng, T., Huang, C., and Zhang, X.: Real-time measurement of phase partitioning of organic compounds using a proton-transfer-reaction time-of-flight mass spectrometer coupled to a CHARON inlet, Atmos. Meas. Tech., 16, 15–28, https://doi.org/10.5194/amt-16-15-2023, 2023.

Piel, F., Müller, M., Mikoviny, T., Pusede, S. E., and Wisthaler, A.: Airborne measurements of particulate organic matter by proton-transfer-reaction mass spectrometry (PTR-MS): a pilot study, Atmos. Meas. Tech., 12, 5947–5958, https://doi.org/10.5194/amt-12-5947-2019, 2019.

Pye, H., Ward-Caviness, C., Murphy, B., Appel, W., and Seltzer, K.: Secondary organic aerosol association with cardiorespiratory disease mortality in the United States, Nat. Commun., 12, 1-8, https://doi.org/10.1038/s41467-021-27484-1, 2021.

https://doi.org/10.5194/egusphere-2025-2331
Preprint. Discussion started: 25 June 2025

Riva, M., Budisulistiorini, S. H., Chen, Y., Zhang, Z., D'Ambro, E. L., Zhang, X., Gold, A., Turpin, B. J., Thornton, J. A., Canagaratna, M. R., and Surratt, J. D.: Chemical Characterization of Secondary Organic Aerosol from Oxidation of Isoprene Hydroxyhydroperoxides, Environ. Sci. Technol., 50, 9889–9899, https://doi.org/10.1021/acs.est.6b02511, 2016.

Robinson, N. H., Hamilton, J. F., Allan, J. D., Langford, B., Oram, D. E., Chen, Q., Docherty, K., Farmer, D. K., Jimenez, J. L., Ward, M. W., Hewitt, C. N., Barley, M. H., Jenkin, M. E., Rickard, A. R., Martin, S. T., McFiggans, G., and Coe, H.: Evidence for a significant proportion of Secondary Organic Aerosol from isoprene above a maritime tropical forest, Atmos. Chem. Phys., 11, 1039–1050, https://doi.org/10.5194/acp-11-1039-2011, 2011.

Roldin, P., Ehn, M., Kurtén, T., Olenius, T., Rissanen, M. P., Sarnela, N., Elm, J., Rantala, P., Hao, L., Hyttinen, N., Heikkinen, L., Worsnop, D. R., Pichelstorfer, L., Xavier, C., Clusius, P., Öström, E., Petäjä, T., Kulmala, M., Vehkamäki, H., Virtanen, A., Riipinen, I., and Boy, M.: The role of highly oxygenated organic molecules in the Boreal aerosol-cloud-climate system, Nat. Commun., 10, 4370, https://doi.org/10.1038/s41467-019-12338-8, 2019.

de Sá, S. S., Palm, B. B., Campuzano-Jost, P., Day, D. A., Hu, W., Isaacman-VanWertz, G., Yee, L. D., Brito, J., Carbone, S., Ribeiro, I. O., Cirino, G. G., Liu, Y., Thalman, R., Sedlacek, A., Funk, A., Schumacher, C., Shilling, J. E., Schneider, J., Artaxo, P., Goldstein, A. H., Souza, R. A. F., Wang, J., McKinney, K. A., Barbosa, H., Alexander, M. L., Jimenez, J. L., and Martin, S. T.: Urban influence on the concentration and composition of submicron particulate matter in central Amazonia, Atmos. Chem. Phys., 18, 12185–12206, https://doi.org/10.5194/acp-18-12185-2018, 2018.

Schulz, C., Schneider, J., Amorim Holanda, B., Appel, O., Costa, A., de Sá, S. S., Dreiling, V., Fütterer, D., Jurkat-Witschas, T., Klimach, T., Knote, C., Krämer, M., Martin, S. T., Mertes, S., Pöhlker, M. L., Sauer, D., Voigt, C., Walser, A., Weinzierl, B., Ziereis, H., Zöger, M., Andreae, M. O., Artaxo, P., Machado, L. A. T., Pöschl, U., Wendisch, M., and Borrmann, S.: Aircraft-based observations of isoprene-epoxydiol-derived secondary organic aerosol (IEPOX-SOA) in the tropical upper troposphere over the Amazon region, Atmos. Chem. Phys., 18, 14979–15001, https://doi.org/10.5194/acp-18-14979-2018, 2018.

Schwantes, R. H., Charan, S. M., Bates, K. H., Huang, Y., Nguyen, T. B., Mai, H., Kong, W., Flagan, R. C., and Seinfeld, J. H.: Low-volatility compounds contribute significantly to isoprene secondary organic aerosol (SOA) under high-NO_x conditions, Atmos. Chem. Phys., 19, 7255–7278, https://doi.org/10.5194/acp-19-7255-2019, 2019.

Seinfeld, J. H. and Pankow, J. F.: Organic Atmospheric Particulate Material, Annu. Rev. Phys. Chem., 54, 121–140, https://doi.org/10.1146/annurev.physchem.54.011002.103756, 2003.

Shrivastava, M., Cappa, C. D., Fan, J., Goldstein, A. H., Guenther, A. B., Jimenez, J. L., Kuang, C., Laskin, A., Martin, S. T., Ng, N. L., Petaja, T., Pierce, J. R., Rasch, P. J., Roldin, P., Seinfeld, J. H., Shilling, J., Smith, J. N., Thornton, J. A., Volkamer, R., Wang, J., Worsnop, D. R., Zaveri, R. A., Zelenyuk, A., and Zhang, Q.: Recent

https://doi.org/10.5194/egusphere-2025-2331
Preprint. Discussion started: 25 June 2025

advances in understanding secondary organic aerosol: Implications for global climate forcing, Rev. Geophys., 55, 509–559, https://doi.org/https://doi.org/10.1002/2016RG000540, 2017.

Shrivastava, M., Andreae, M. O., Artaxo, P., Barbosa, H. M. J., Berg, L. K., Brito, J., Ching, J., Easter, R. C., Fan, J., Fast, J. D., Feng, Z., Fuentes, J. D., Glasius, M., Goldstein, A. H., Alves, E. G., Gomes, H., Gu, D., Guenther, A., Jathar, S. H., Kim, S., Liu, Y., Lou, S., Martin, S. T., McNeill, V. F., Medeiros, A., de Sá, S. S., Shilling, J. E., Springston, S. R., Souza, R. A. F., Thornton, J. A., Isaacman-VanWertz, G., Yee, L. D., Ynoue, R., Zaveri, R. A., Zelenyuk, A., and Zhao, C.: Urban pollution greatly enhances formation of natural aerosols over the Amazon rainforest, Nat. Commun., 10, 1046, https://doi.org/10.1038/s41467-019-08909-4, 2019.

Slowik, J. G., Brook, J., Chang, R. Y.-W., Evans, G. J., Hayden, K., Jeong, C.-H., Li, S.-M., Liggio, J., Liu, P. S. K., McGuire, M., Mihele, C., Sjostedt, S., Vlasenko, A., and Abbatt, J. P. D.: Photochemical processing of organic aerosol at nearby continental sites: contrast between urban plumes and regional aerosol, Atmos. Chem. Phys., 11, 2991–3006, https://doi.org/10.5194/acp-11-2991-2011, 2011.

Song, J., Saathoff, H., Jiang, F., Gao, L., Zhang, H., and Leisner, T.: Sources of organic gases and aerosol particles and their roles in nighttime particle growth at a rural forested site in southwest Germany, Atmos. Chem. Phys., 24, 6699–6717, https://doi.org/10.5194/acp-24-6699-2024, 2024.

Srivastava, D., Vu, T. V., Tong, S., Shi, Z., and Harrison, R. M.: Formation of secondary organic aerosols from anthropogenic precursors in laboratory studies, npj Clim. Atmos. Sci., 5, 22, https://doi.org/10.1038/s41612-022-00238-6, 2022.

Surratt, J. D., Murphy, S. M., Kroll, J. H., Ng, N. L., Hildebrandt, L., Sorooshian, A., Szmigielski, R., Vermeylen, R., Maenhaut, W., Claeys, M., Flagan, R. C., and Seinfeld, J. H.: Chemical Composition of Secondary Organic Aerosol Formed from the Photooxidation of Isoprene, J. Phys. Chem. A, 110, 9665–9690, https://doi.org/10.1021/jp061734m, 2006.

Surratt, J. D., Chan, A. W. H., Eddingsaas, N. C., Chan, M., Loza, C. L., Kwan, A. J., Hersey, S. P., Flagan, R. C., Wennberg, P. O., and Seinfeld, J. H.: Reactive intermediates revealed in secondary organic aerosol formation from isoprene, Proc. Natl. Acad. Sci. USA, 107, 6640–6645, https://doi.org/10.1073/pnas.0911114107, 2010.

Tasoglou, A. and Pandis, S. N.: Formation and chemical aging of secondary organic aerosol during the β-caryophyllene oxidation, Atmos. Chem. Phys., 15, 6035–6046, https://doi.org/10.5194/acp-15-6035-2015, 2015.

Tröstl, J., Chuang, W. K., Gordon, H., Heinritzi, M., Yan, C., Molteni, U., Ahlm, L., Frege, C., Bianchi, F., Wagner, R., Simon, M., Lehtipalo, K., Williamson, C., Craven, J. S., Duplissy, J., Adamov, A., Almeida, J., Bernhammer, A.-K., Breitenlechner, M., Brilke, S., Dias, A., Ehrhart, S., Flagan, R. C., Franchin, A., Fuchs, C., Guida, R., Gysel, M., Hansel, A., Hoyle, C. R., Jokinen, T., Junninen, H., Kangasluoma, J., Keskinen, H., Kim, J., Krapf, M., Kürten, A., Laaksonen, A., Lawler, M., Leiminger, M., Mathot, S., Möhler, O., Nieminen, T., Onnela, A., Petäjä, T., Piel, F. M., Miettinen, P., Rissanen, M. P., Rondo, L., Sarnela, N., Schobesberger, S.,

https://doi.org/10.5194/egusphere-2025-2331
Preprint. Discussion started: 25 June 2025

Sengupta, K., Sipilä, M., Smith, J. N., Steiner, G., Tomè, A., Virtanen, A., Wagner, A. C., Weingartner, E., Wimmer, D., Winkler, P. M., Ye, P., Carslaw, K. S., Curtius, J., Dommen, J., Kirkby, J., Kulmala, M., Riipinen, I., Worsnop, D. R., Donahue, N. M., and Baltensperger, U.: The role of low-volatility organic compounds in initial particle growth in the atmosphere, Nature, 533, 527–531, https://doi.org/10.1038/nature18271, 2016.

Wennberg, P. O., Bates, K. H., Crounse, J. D., Dodson, L. G., McVay, R. C., Mertens, L. A., Nguyen, T. B., Praske, E., Schwantes, R. H., Smarte, M. D., St Clair, J. M., Teng, A. P., Zhang, X., and Seinfeld, J. H.: Gas-Phase Reactions of Isoprene and Its Major Oxidation Products, Chem. Rev., 118, 3337–3390, https://doi.org/10.1021/acs.chemrev.7b00439, 2018.

Worton, D. R., Moreno, S., O'Daly, K., and Holzinger, R.: Development of an International System of Units (SI)-traceable transmission curve reference material to improve the quantitation and comparability of proton-transfer-reaction mass-spectrometry measurements, Atmos. Meas. Tech., 16, 1061–1072, https://doi.org/10.5194/amt-16-1061-2023, 2023.

Xu, L., Kollman, M. S., Song, C., Shilling, J. E., and Ng, N. L.: Effects of NO_x on the Volatility of Secondary Organic Aerosol from Isoprene Photooxidation, Environ. Sci. Technol., 48, 2253–2262, https://doi.org/10.1021/es404842g, 2014.

Xu, L., Suresh, S., Guo, H., Weber, R. J., and Ng, N. L.: Aerosol characterization over the southeastern United States using high-resolution aerosol mass spectrometry: spatial and seasonal variation of aerosol composition and sources with a focus on organic nitrates, Atmos. Chem. Phys., 15, 7307–7336, https://doi.org/10.5194/acp-15-7307-2015, 2015a.

Xu, L., Guo, H., Boyd, C. M., Klein, M., Bougiatioti, A., Cerully, K. M., Hite, J. R., Isaacman-VanWertz, G., Kreisberg, N. M., Knote, C., Olson, K., Koss, A., Goldstein, A. H., Hering, S. V, de Gouw, J., Baumann, K., Lee, S.-H., Nenes, A., Weber, R. J., and Ng, N. L.: Effects of anthropogenic emissions on aerosol formation from isoprene and monoterpenes in the southeastern United States, Proc. Natl. Acad. Sci. USA, 112, 37–42, https://doi.org/10.1073/pnas.1417609112, 2015b.

Yáñez-Serrano, A. M., Bourtsoukidis, E., Alves, E. G., Bauwens, M., Stavrakou, T., Llusià, J., Filella, I., Guenther, A., Williams, J., Artaxo, P., Sindelarova, K., Doubalova, J., Kesselmeier, J., and Peñuelas, J.: Amazonian biogenic volatile organic compounds under global change, Glob. Chang. Biol., 26, 4722–4751, https://doi.org/https://doi.org/10.1111/gcb.15185, 2020.

Zhang, H., Surratt, J. D., Lin, Y. H., Bapat, J., and Kamens, R. M.: Effect of relative humidity on SOA formation from isoprene/NO photooxidation: enhancement of 2-methylglyceric acid and its corresponding oligoesters under dry conditions, Atmos. Chem. Phys., 11, 6411–6424, https://doi.org/10.5194/acp-11-6411-2011, 2011.

Zhang, H., Yee, L. D., Lee, B. H., Curtis, M. P., Worton, D. R., Isaacman-VanWertz, G., Offenberg, J. H., Lewandowski, M., Kleindienst, T. E., Beaver, M. R., Holder, A. L., Lonneman, W. A., Docherty, K. S., Jaoui,

https://doi.org/10.5194/egusphere-2025-2331
Preprint. Discussion started: 25 June 2025

M., Pye, H. O. T., Hu, W., Day, D. A., Campuzano-Jost, P., Jimenez, J. L., Guo, H., Weber, R. J., de Gouw, J., Koss, A. R., Edgerton, E. S., Brune, W., Mohr, C., Lopez-Hilfiker, F. D., Lutz, A., Kreisberg, N. M., Spielman, S. R., Hering, S. V, Wilson, K. R., Thornton, J. A., and Goldstein, A. H.: Monoterpenes are the largest source of summertime organic aerosol in the southeastern United States, Proc. Natl. Acad. Sci. USA, 115, 2038–2043, https://doi.org/10.1073/pnas.1717513115, 2018.

Zhang, J., Huff Hartz, K. E., Pandis, S. N., and Donahue, N. M.: Secondary Organic Aerosol Formation from Limonene Ozonolysis: Homogeneous and Heterogeneous Influences as a Function of NO_x, J. Phys. Chem. A, 110, 11053–11063, https://doi.org/10.1021/jp062836f, 2006.

Zhang, Q., Jimenez, J. L., Canagaratna, M. R., Ulbrich, I. M., Ng, N. L., Worsnop, D. R., and Sun, Y.: Understanding atmospheric organic aerosols via factor analysis of aerosol mass spectrometry: a review, Anal. Bioanal. Chem., 401, 3045–3067, https://doi.org/10.1007/s00216-011-5355-y, 2011.

Zhang, Y., Chen, Y., Lei, Z., Olson, N. E., Riva, M., Koss, A. R., Zhang, Z., Gold, A., Jayne, J. T., Worsnop, D. R., Onasch, T. B., Kroll, J. H., Turpin, B. J., Ault, A. P., and Surratt, J. D.: Joint Impacts of Acidity and Viscosity on the Formation of Secondary Organic Aerosol from Isoprene Epoxydiols (IEPOX) in Phase Separated Particles, ACS Earth Sp. Chem., 3, 2646–2658, https://doi.org/10.1021/acsearthspacechem.9b00209, 2019.

Zhou, P., Ganzeveld, L., Taipale, D., Rannik, Ü., Rantala, P., Rissanen, M. P., Chen, D., and Boy, M.: Boreal forest BVOC exchange: emissions versus in-canopy sinks, Atmos. Chem. Phys., 17, 14309–14332, https://doi.org/10.5194/acp-17-14309-2017, 2017.